frontiers in Marine Science

ORIGINAL RESEARCH
published: 07 March 2022
doi: 10.3389/fmars.2022.847600

Taxonomy and Phylogeny of Two Tintinnid Ciliates of *Leprotintinnus* (Protista, Ciliophora, Choreotrichida) Combining the Loricae, Cytological, Ontogenetic Features, and Barcoding Genes

Tao Hu[1†], Zhaoyi Wang[1†], Weiwei Liu[2] and Xiaofeng Lin[3]*

[1] Laboratory of Protozoology, Guangzhou Key Laboratory of Subtropical Biodiversity and Biomonitoring, South China Normal University, Guangzhou, China, [2] Key Laboratory of Tropical Marine Bio-Resources and Ecology, South China Sea Institute of Oceanology, Chinese Academy of Sciences, Guangzhou, China, [3] Key Laboratory of the Ministry of Education for Coastal and Wetland Ecosystem, The Fujian Provincial Key Laboratory for Coastal Ecology and Environmental Studies, College of the Environment and Ecology, Xiamen University, Xiamen, China

OPEN ACCESS

Edited by:
Zhijun Dong,
Yantai Institute of Coastal Zone Research (CAS), China

Reviewed by:
Susumu Ohtsuka,
Hiroshima University, Japan
Yong Jiang,
Ocean University of China, China

***Correspondence:**
Xiaofeng Lin
linxf@xmu.edu.cn

[†] These authors share first authorship

Specialty section:
This article was submitted to Marine Evolutionary Biology, Biogeography and Species Diversity, a section of the journal Frontiers in Marine Science

Received: *03 January 2022*
Accepted: *07 February 2022*
Published: *07 March 2022*

Citation:
Hu T, Wang Z, Liu W and Lin X (2022) Taxonomy and Phylogeny of Two Tintinnid Ciliates of Leprotintinnus (Protista, Ciliophora, Choreotrichida) Combining the Loricae, Cytological, Ontogenetic Features, and Barcoding Genes. Front. Mar. Sci. 9:847600. doi: 10.3389/fmars.2022.847600

Tintinnid ciliates are a highly diverse and essential group in the marine planktonic microbial loop. However, most of the known tintinnids were recorded only by the lorica characters and very few of them had been studied on their cytological features. In this study, the morphological characters of the lorica, ciliary pattern, nuclear apparatus, ontogenesis, and the molecular phylogeny of two poorly known tintinnid ciliates, *Leprotintinnus nordqvisti* (Brandt, 1906) Kofoid and Campbell (1929) and *L. simplex* Schmidt (1902), isolated from coastal waters of southern China, were investigated based on living observation, silver staining, three nuclear ribosomal DNA markers (18S, ITS1-5.8S-ITS2, and 28S genes) and one mitochondrial DNA marker (*CO1* gene). For the first time, the somatic ciliary pattern of the genus *Leprotintinnus* was disclosed, *viz*., comprising a ventral, a dorsal, and a posterior kinety as well as a right, a left, and a lateral ciliary field. The diagnoses of both *Leprotintinnus* species were improved and the neotype was assigned. The ontogenesis of *L. nordqvisti* was in enantiotropic division mode with the new dorsal and posterior kineties generated *de novo*. The molecular phylogeny confirmed that *Leprotintinnus* species are closely related to some species of *Tintinnopsis*, *Stylicauda*, *Rhizodomus*, and *Climacocylis*. The anterior extending of the ventral kinety together with some of the lateral kinety is likely to be a distinguishing feature to determine their systematic relationships. This study also revealed that (i) the lorica of *L. nordqvisti* is polymorphic or plastic; (ii) *Leprotintinnus tubulosus* Roxas (1941) might be a synonym of *L. nordqvisti*; (iii) *Leprotintinnus neriticus* sensu Yoo et al. (1988) might be a misidentification of *L. simplex*.

Keywords: *Leprotintinnus nordqvisti*, *Leprotintinnus simplex*, *Leprotintinnus tubulosus*, *Leprotintinnus neriticus*, neotype, ontogenesis

INTRODUCTION

Tintinnids (Ciliophora, Oligotrichea, Choreotrichida) are unique planktonic ciliates with lorica as a cell house (Adl et al., 2019). They are essential transmitters of material and energy in the marine planktonic microbial loop, by preying on phytoplankton and being preyed on by small zooplankton or fish larvae (Dolan et al., 2013; Zingel et al., 2019). Since the first record in Müller (1776), over 1,000 tintinnid species have been reported. Most of them were found in marine habitats (Kofoid and Campbell, 1929, 1939; Liu et al., 2020), and a few species occurred in brackish waters (Sniezek et al., 1991; Snyder and Brownlee, 1991; Smith et al., 2018) or fresh waters (Foissner and O'Donoghue, 1990; Petz and Foissner, 1993). The taxonomic classification of most known tintinnids solely relied on their loricae features. While the lorica is useful for species discrimination only in some cases such as ecological studies (Santoferrara et al., 2013), a huge body of literature have found that different types of loricae (polymorphism or plasticity) could be owned by the same species in the laboratory pure cultures (Gold and Morales, 1974, 1975; Laval-Peuto, 1977, 1981). Different DNA sequences were also obtained from two almost identical lorica forms (cryptic species) in field samples (Xu et al., 2012; Santoferrara et al., 2015). Hence, the lorica-based taxonomy is clearly outdated and might be unreliable compared to the cytological features (Dolan, 2016).

The ciliary pattern is one of the most important cytological features for ciliate identification, but it has been reported for less than 3% of known tintinnids (Santoferrara and McManus, 2021). Molecular data, such as 18S rDNA, ITS rDNA, etc., can supply crucial support for species discrimination of closely related ciliates. However, some variations of lorica features were not verified in the phylogenetic analysis based on gene sequences (Santoferrara et al., 2017). Therefore, it is necessary to find more comprehensive morphological features and combine them with molecular phylogeny in order to improve the specific resolution of tintinnids (Agatha and Strüder-Kypke, 2012; Santoferrara et al., 2016).

The tintinnid genus *Leprotintinnus* was established based on the features of lorica, namely open at both ends, surface viscous, soft, and often sparsely agglutinated (Jörgensen, 1900). *Leprotintinnus pellucidus* (Cleve, 1899) Jörgensen, 1901 was designated as the type species by Kofoid and Campbell (1929). This *Leprotintinnus* was considered a member of the family Tintinnidiidae for a long time because of its soft and often sparsely agglutinated loricae. Zhang et al. (2017) and Santoferrara et al. (2017) assigned this genus to *Incertae sedis* in tintinnid according to their phylogeny analysis and unclear lorica-based morphological affinity. However, this removal has not yet been confirmed by morphological features, i.e., the ciliary pattern of this genus. To date, about ten *Leprotintinnus* species have been recorded from coastal or fresh waters, but none of the ciliary patterns were reported.

In the present work, two *Leprotintinnus* species, namely *Leprotintinnus nordqvisti* (Brandt, 1906) Kofoid and Campbell, 1929 and *Leprotintinnus simplex* Schmidt (1902), collected from coastal waters of southern China, were investigated using detailed live observation, silver staining, and DNA sequencing. The cytological features of this genus were revealed for the first time. The purpose of this study was to improve our understanding of the chaotic taxonomy and phylogeny of tintinnids by combining features of the lorica, ciliary patterns, and barcoding genes.

MATERIALS AND METHODS

Sample Collection, Observation, and Identification

Both species were collected from surface water (0–2 m water depth) using 20-μm mesh plankton nets. *Leprotintinnus nordqvisti* was found in an oyster farm in Yangjiang, Guangdong Province, China in November 2019 (salinity 27‰, pH 8.1, and water temperature 23.5°C). *Leprotintinnus simplex* was isolated from Yuandang Lake in Xiamen, Fujian Province, China in December 2020 (salinity 28‰, pH 8.1, and water temperature 21.7°C). Both species were isolated and observed in the Petri dishes of 10 cm diameter with a water depth of about 8 mm, under a stereoscopic microscope (Guiguang XTL-400) at room temperature. Living morphology was investigated under an optical microscope (Nikon 80i) equipped with a digital camera. The protargol silver-staining method was used to reveal the ciliary pattern and the nuclear apparatus (Ji and Wang, 2018). The protargol powder was manually synthesized following the method described by Pan et al. (2013). Counts and measurements on stained cells were performed at 1,000×, while *in vivo* measurements were done at 400–1,000×. Drawings of live specimens were based on mean measurements, while those of stained specimens were performed with the aid of a camera lucida. Terminology is mainly according to the study of Agatha and Riedel-Lorjé (2006). The classification follows the study conducted by Santoferrara and McManus (2021).

Neotype Materials

In view of the requirements of Article 75.3.6 of the International Code of Zoological Nomenclature (International Code of Zoological Nomenclature [ICZN], 1999), we designated the neotypes for *L. nordqvisti* and *L. simplex*, because (i) no type specimens are available for either species; (ii) the original descriptions lack detailed cytological and morphometric features; (iii) the neotype specimens are clearly described and illustrated, allowing for the clear identification of specific features. Unfortunately, neither of the neotypes is collected from the original type locality (coastal waters of southern China for the neotype populations vs. Brazilian coast water for *L. nordqvisti* and the Gulf of Siam for *L. simplex*). Nevertheless, it seems reasonable to designate neotypes from similar coastal habitats and necessary in order to provide stability in tintinnid taxonomy, following the argumentation of Foissner (2002), Corliss (2003).

DNA Extraction, PCR Amplification, and Sequencing

Cells for DNA extraction were isolated and rinsed five times with filtered (0.22 μm pore size) habitat water. Total genomic DNA was extracted from every single cell, using the DNeasy Blood

& Tissue kit (Qiagen, Mississauga, ON, Canada), following the manufacturer's protocol. Cells of *L. nordqvisti* in different lorica forms, i.e., with or without an aboral flare, were separated and recorded in DNA extraction. PCR amplifications of barcoding genes (18S, ITS1-5.8S-ITS2, 28S, and *CO1*) were done using respective primers, including EukA (5′-AAC CTG GTT GAT CCT GCC AGT-3′) (Medlin et al., 1988), 82F (5′-GAA ACT GCG AAT GGC TC-3′) (Jerome et al., 1996), EukB (5'-TGA TCC TTC TGC AGG TTC ACC TAC-3') (Medlin et al., 1988), R2 (5'-AAC CTT GGA GAC CTG AT-3') (Moreira et al., 2007), and 28S rev2 (5′-ACG ATC GAT TTG CAC GTC AG-3′) (Sonnenberg et al., 2007) for rDNA sequences, CiCO1 Fv2 (5′-GWT GRG CKA TGA TYA CAC C-3′) and CiCO1 Rv2 (5′-ACC ATR TAC ATA TGA TGW CC-3′) for *CO1* sequences (Park et al., 2018). The PCR amplifications were performed using Q5®Hot Start High-Fidelity DNA Polymerase (New England BioLabs, United States) to minimize the possibility of PCR amplification errors at the standard PCR protocol. The products of PCR reactions were directly sequenced in both directions using ABI 3730 sequencer by the Tianyi Huiyuan Bioscience and Technology Incorporation (Guangzhou, China).

Phylogenetic Analyses

In addition to the newly obtained sequences, other sequences used for phylogenetic analyses were downloaded from the GenBank. *Oxytricha ferruginea* (AF370027) and *O. granulifera* (AF164122) were taken as the outgroup taxa in the 18S rDNA phylogenetic tree. *Urostyla grandis* (AF508781), *Stylonychia lemnae* (AF508773), and *Hemiurosomoida longa* (AF508763) were used as the outgroup taxa in the ITS1-5.8s rDNA-ITS2 phylogeny analysis. *Hemiurosomoida longa* (AF508763) and *Stylonychia mytilus* (AF508774) were the outgroup taxa in our 28S rDNA phylogenetic tree. *Euplotes vannus* (MG594918) and *Diophrys appendiculata* (MG594867) were the outgroup taxa in the *CO1* gene phylogeny analysis.

The sequences were aligned with MAFFT version 7.313 (Katoh and Standley, 2013). Ambiguous positions were removed using Gblocks version 0.91b (Talavera and Castresana, 2007) with the default parameters. The final alignments comprised of 89 18S rDNA sequences with 1637 bp, 61 ITS1-5.8S-ITS2 region sequences with 481 bp, 61 28S rDNA sequences with 656 bp, and 20 *CO1* gene sequences with 478 bp, respectively. ModelFinder was used to select the best-fit model using Akaike Information Criterion (Kalyaanamoorthy et al., 2017). Maximum likelihood (ML) analyses were inferred using IQ-TREE (Nguyen et al., 2015) under the model of GTR+R3+F (18S rDNA), SYM+R6 (ITS1-5.8S-ITS2), TN+R7+F (28S rDNA), and GTR+G4+F (*CO1*), respectively for 5,000 ultrafast bootstraps (Minh et al., 2013). Bayesian Inference (BI) analyses were executed with MrBayes version 3.2.6 (Ronquist et al., 2012) under the model of GTR+G+F (*CO1*) and GTR+I+G+F (18S rDNA, ITS1-5.8S-ITS2 and 28S rDNA), respectively. Two parallel runs were performed. Four simultaneous Markov chain Monte Carlo simulations (MCMC) were run for 2,000,000 generations with a sampling frequency of 100 generations and a burn-in of the initial 25% trees. Tree visualization was done in MEGA version 7.0.2 (Kumar et al., 2016) and Adobe Photoshop CC 2017. Pairwise distances were calculated by MEGA version 7.0.2 with the *P*-distance model (Kumar et al., 2016).

RESULTS

Class Oligotrichea Bütschli, 1889
Order Choreotrichida Small and Lynn, 1985
Suborder Tintinnina Kofoid and Campbell, 1929
Genus *Leprotintinnus* Jörgensen, 1900

Leprotintinnus nordqvisti (Brandt, 1906) Kofoid and Campbell, 1929

Improved Diagnosis of *Leprotintinnus nordqvisti*

Remark. This diagnosis is improved based only on the original and the present populations, but no other known population included considering their uncertainty of species identification only based on lorica characters (e.g., Wang and Nie, 1932; Hada, 1938, 1974; Yoo et al., 1988).

Loricae cylindrical, about 80–200 μm long, anterior end slightly flared with opening 30–46 μm across, and posterior end contracted or distinctly widened with opening 28–60 μm across. Cells obconical, *in vivo* about 33–95 × 30–49 μm. Usually two (1–3) macronuclear nodules. Ventral kinety is usually anteriorly extremely close to the collar membranes and commencing from the fifth or sixth kinety of the right ciliary field. The right ciliary field comprises 14 kineties on average, left ciliary field comprises 11 kineties on average. Lateral ciliary field comprising 17 kineties on average, the anterior parts of the rightmost kinety of the lateral ciliary field anterior extended and curving rightwards parallel to the ventral kinety. One dorsal kinety is composed of 34 dikinetids on average. One posterior kinety, with about 15 dikinetids, is positioned below the sixth or seventh kinety of the left ciliary field. One buccal membranelle. On average 21 collar membranelles, four of them elongated into the buccal cavity.

Neotype of *Leprotintinnus nordqvisti*

This species was originally discovered on the Brazilian coast (Brandt, 1906). No information on the holotype is available. Hence a neotype should be assigned. The neotype population was sampled from an oyster farm in Yangjiang, southern China (111°55′26″E, 21°39′49″N). One protargol-stained slide (registration number: HT2019112261a) including the neotype (marked with a black circle) and seven slides (registration numbers: HT2019112261b-g) with voucher specimens were deposited in the Laboratory of Protozoology, Ocean University of China, Qingdao, China.

Morphological Description of *Leprotintinnus nordqvisti*

Loricae cylindrical, sometimes slightly curved, about 80–185 μm long (**Figures 1A,D**, **2A–F** and **Table 1**). Lorica is opening at both ends. The oral margin slightly flared with an irregular opening rim 37–46 μm across, with a ratio of lorica length to anterior aperture diameter 2–4.2:1. The posterior end of the loricae is unstable, broken, contracted, or distinctly widened, about 28–45 μm in diameter. Lorica walls are roughly transparent, soft,

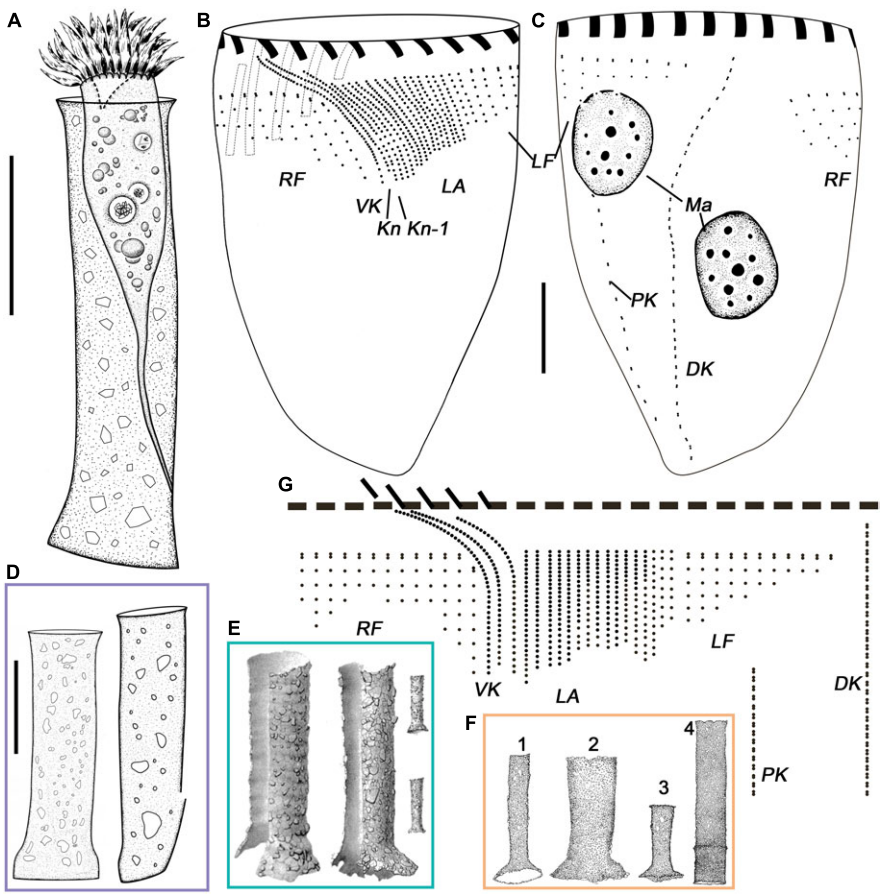

FIGURE 1 | *Leprotintinnus nordqvisti* from life **(A,D–F)** and after protargol staining **(B,C,G)**. **(A)** A typical individual. **(B,C)** The ciliary pattern of ventral and dorsal sides of the same specimen. **(D)** Different shapes of loricae with agglomerated mineral particles. **(E)** Lateral view of loricae from Brandt (1906). **(F)** *L. nordqvisti* from Roxas (1941) (except for 4, original named *L. tubulosus*). **(G)** Kinetal map of a morphostatic specimen. DK, dorsal kinety; K_n, the last kinety of the lateral ciliary field; K_{n-1}, the penultimate kinety of the lateral ciliary field; LA, lateral ciliary field; LF, left ciliary field; Ma, macronuclear nodules; RF, right ciliary field; VK, ventral kinety. Scale bars: 20 μm.

sparsely agglutinated with irregular particles, which are about 2–7 μm long (**Figures 1D**, **2G,H**).

Fully extended cells usually 55–68 × 28–32 μm in size and elongated obconical shaped. After protargol staining, specimens about 33–95 × 30–49 μm in size. Posterior cell proper merging gradually into a slender, wrinkled, and highly contractile peduncle (stalk). Peduncle up to 30 μm long and attached to the inner wall of lorica at posterior 20 to 30% (**Figures 1A**, **2A–C,F** and **Table 1**). Contracted cells about 40–50 × 30–35 μm *in vivo* (**Figure 2F**). When disturbed, cells retract quickly into loricae with its contractile stalk and a posterior portion or likely escape from loricae with the naked trophont barrel-shaped, about 31–40 × 25–35 μm in size (**Figure 2K**). Usually two (1–3) ellipsoidal or ovoidal macronuclear nodules, about 7–26 × 7–20 μm in diameter, with nucleoli 2–4 μm across after protargol staining; anterior nodule 6–17 μm posteriorly to the anterior end of the cell. One or two micronuclei attached or near to macronuclear nodules, about 2 μm across (**Figures 1C**, **3H–J**). Neither striae, tentaculoids, accessory comb, contractile vacuole, cytopyge, nor capsule were observed. Cytoplasm colorless, sometimes with several food vacuoles up to 5 μm across containing ingested yellow microalgae (**Figures 2A–C,F,J,K**). Swimming by rotation about the main cell axis.

The somatic ciliary pattern in the most complex type (Agatha and Strüder-Kypke, 2007), i.e., comprising a ventral, a dorsal, and a posterior kinety as well as a right, a left, and a lateral ciliary field (**Figures 1B,C,G**, **3A–E** and **Table 1**). Kinetids of each ciliary row are ostensibly connected by argyrophilic fibers (**Figures 3A–E**). Ventral kinety anterior is extremely adjacent to the collar membranelles, commencing from the fifth or sixth kinety of the right ciliary field. Ventral kinety curving leftwards and extending downward parallel to kineties of the lateral ciliary field, and terminated at anterior 40% of the cell, with 25–53 ciliated monokinetids, anterior kinetosomes closely spaced, but more widely spaced in posterior portion, with cilia about 2 μm long after impregnation (**Figures 1B,G**, **3A,B**). The right ciliary field includes 13–15 kineties, commencing at the same level (about 5–10 μm below collar membranelles) except for the first kinety which commences about 8–14 μm below collar membranelles. The kinety in the right ciliary field is about 6–16 μm long,

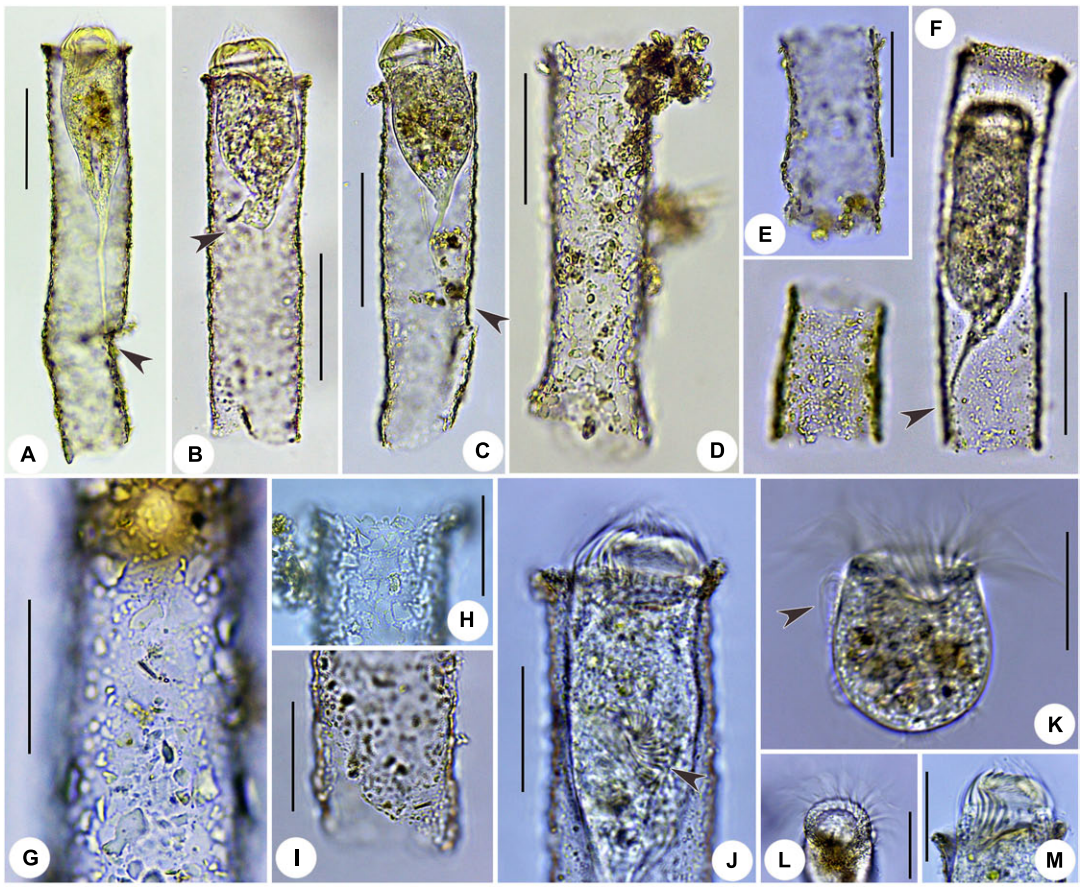

FIGURE 2 | *Leprotintinnus nordqvisti in vivo*. **(A–F)** Showing the variability of loricae shape and size, the arrows indicate the positions where the cell is properly attached to the inner wall of the lorica via the peduncle. **(G)** Lorica wall with numerous mineral particles. **(H)** Slightly flared oral marginal. **(I)** Broken aboral end opening. **(J)** Not fully contracted specimen, arrowhead denotes the oral primordium. **(K)** Cell proper out of the lorica, arrowhead denotes the elongated anteriormost cilia. **(L)** Oblique top view showing the oral membranelles. **(M)** Ventral view of cell showing the oral cavity. Scale bars: 50 μm **(A–F)**, 30 μm **(G–M)**.

spaced about 2 μm apart, composed of 4–11 monokinetics and one anterior dikinetid (**Figures 1B,C,G**, **3A,E**). Cilia of the right ciliary field about 2–3 μm long after protargol impregnation, except for conspicuously long ones in the rightmost several kineties (about 8–12 μm long) and the anterior cilium of each dikinetids (about 15–20 μm long) (**Figures 3A,E**). Dorsal kinety commencing about 4–8 μm posteriorly to collar membranelles, about 7–14 μm from the left ciliary fields, about 4–7 μm from the right ciliary fields, and curving leftwards slightly and terminated at the posterior end of the cell. Dorsal kinety about 45–72 μm long, with 25–43 dikinetids (**Figures 1B,C,G**, 3C,E). Cilia is associated only with each posterior dikinetidal basal body, 5–8 μm long after protargol impregnation (**Figures 3C,E**). The left ciliary field including 10–12 kineties, commencing about 5–12 μm below the collar membranelles, about 1–12 μm long, spaced about 2 μm apart, composed of 1–7 monokinetids and one anterior dikinetid, but the first kinety often consisting of only one anterior dikinetid (**Figures 1B,C,G**, **3C–E**). Cilia of the left ciliary field about 6–8 μm long after protargol impregnation, except for the anterior cilia of dikinetids measuring about 15 μm (**Figures 3C–E**). The lateral ciliary field includes 16–19 kineties, commencing about 3–8 μm below the collar membranelles, except for (i) the last kinety (K_n) commencing anteriorly from the fourth or fifth kinety of the right ciliary field (about 1–2 μm posterior to the collar membranelles) and extending parallel to the ventral kinety, and (ii) the penultimate kinety (K_{n-1}) commencing anterior from the second or third kinety of the right ciliary field, about 3–5 μm posterior to the collar membranelles, with anterior end lower than that of K_n but higher than that of other kineties; clockwise inclined, spaced about 1 μm apart, composed of densely spaced monokinetids, kinetids and kineties more densely spaced in right portion than those in left field portion, and kinetids more widely spaced in the posterior portion of kineties than those in anterior portion; cilia about 3–4 μm long after protargol impregnation (**Figures 1B,C,G**, **3A,B,D**). The posterior kinety commencing below the sixth or seventh kinety of the left ciliary field, about 21–45 μm posteriorly to the collar membranelles, about 5–12 μm apart from the dorsal kinety, extending almost longitudinally to the posterior end of the cell, about 27–47 μm long, composed of 11–20 dikinetids with cilia about 5–8 μm long (after protargol impregnation) associated only with each posterior basal body (**Figures 1B,C,G**, **3C**).

Oral apparatus occupying anterior cell end (**Figures 2K–M**). Adoral zone of membranelles closed, 31–48 μm across after protargol staining, perpendicular to main cell axis in contracted specimens, composed of 20 or 21 collar membranelles and invariably one buccal membranelle (**Figures 1B,C,G**, **2L,M**, **3C,F,G** and **Table 1**). Collar membranelles up to 8–10 μm long, separated by shallow ridges about 7–8 μm wide, consisting of three rows of basal bodies, with cilia up to 30–35 μm long *in vivo* (**Figures 1B**, **3C**). Polykinetids of proximal-most four collar membranelles successively elongated, extending into a deep buccal cavity about 12–15 μm (**Figures 1B**, **3F**). Single buccal membranelle, with a base about 15 μm long (**Figures 1B**, **3F**). Endoral membrane, extending across the peristomial field and right side of the buccal cavity, composed of a single row of ciliated monokinetids, probably with monostichomonad structure (**Figures 1B**, **3G**). Argyrophilic fibers were barely recognizable.

Ontogenesis of *Leprotintinnus nordqvisti*

Leprotintinnus nordqvisti shows an enantiotropic division mode in which hypoapokinetal somitogenesis occurred in a subsurface pouch in the posterior half of cell proper (**Figures 3K–T**, **4A–I**). In the very early dividers, the oral primordium of the opisthe originates *de novo* and locates in the center of the ventral side, on the left of the posterior ventral kinety end, posteriorly to the lateral ciliary field (**Figures 3K–N**, **4A,B**). Later, with the further proliferation of basal bodies, the anarchic field becomes larger and several membranelles differentiate (**Figures 3L**, **4C**). One replication band emerges in each macronuclear nodules and gradually migrates through the nucleus (**Figure 3L**). Subsequently, the oral primordium rotates clockwise and proliferates rapidly to form a reverse C-shape, while the inner end of each membranelle plunges into the center of the body, with four membranes in the posterior end of the membranelle zone extending inward significantly longer than the other membranes (**Figures 3D–F**, **4D**). The outer ends of the membranelles rotate counterclockwise, and the membranes extend obliquely across the peristomial rim (**Figures 3M**, **4D**). The endoral membranelle is close to the internal edge of the upper membranes and extends across the peristomial field (**Figure 3M**). The two ends of the oral primordium meet to form a closed funnel-shaped membranelles zone of the opisthe, which is perpendicularly orientated to the cells' ventral side (**Figures 3N**, **4F,G**). During the process of ontogenesis, the parental oral apparatus is inherited by the proter, and no reorganization was observed in the parental oral infraciliature.

Basal body proliferation and division of kineties occur firstly in the posterior and dorsal kineties, then in the ventral kinety, then in the right and left ciliary fields, and finally in the lateral ciliary field (**Figures 3O–T**, **4D–I**). In the early dividers, the posterior and dorsal kineties of the opisthe start to originate *de novo* on the right side of the old structures (**Figures 3O**, **4A,B**). And then, the posterior end of the old ventral kinety proliferates and elongates downward along the right of the oral primordium to form the ventral kinety of opisthe (**Figures 3K,L**, **4C**). Subsequently, the somatic kineties of the right and left ciliary fields of the opisthe originate below each one of proter, and elongate downward by intrakinetal proliferation (**Figures 3P,Q**, **4D,E**). In late middle dividers, the lateral ciliary field of opisthe begins to differentiate and proliferate on the posterior-right side of the oral primordium (**Figure 3R**). The argyrophilic structures/fibers appear to connect the corresponding kinety fragments of proter and opisthe in the right and left ciliary fields, while no connection of fibers seems to be observed in the lateral ciliary field (**Figure 3R**). From the middle-to-late stage, the extended ventral kinety breaks apart and differentiates into the ventral kinety of the opisthe (**Figure 3S**). In late middle dividers, the ciliature rows on the ventral sides of the opisthe arranged in a semi-circle around the lower margin of the developing oral primordium (**Figures 3T**, **4F,G**). And the right and left ciliary fields of the opisthe to appear not to be connected to the older structures by argyrophilic structures/fibers anymore (**Figures 3T**, **4F,G**).

One ante divider, i.e., a proter in cell division, was found, given its dividing macronucleus nodule and conspicuous anterior elongation of ventral kinety and penultimate two lateral kineties (**Figures 3C**, **4H,I**). Ontogenesis and reconstruction of the interphase nuclear apparatus are not completed with the separation of proter and opisthe (at least in this division product). Two posterior kinety fragments were found arranged up and down, which may subsequently undergo connection to form the single row of the basal body (**Figures 3C**, **4H,I**).

Leprotintinnus simplex Schmidt, 1902

Improved Diagnosis of *Leprotintinnus simplex*

Remark. This diagnosis is improved based only on the original and the present populations but no other known populations included considering their uncertainty of species identification only based on characters of loricae (e.g., Hada, 1938; Yoo et al., 1988).

Lorica cylindrical, about 170–425 μm long, with gradually tapering aboral end, anterior opening 41–68 μm wide, and posterior opening 30–63 μm across. Two ellipsoidal macronuclear nodules. Ventral kinety is usually anterior commencing from the twelfth or thirteenth kinety of the right ciliary field and closely adjacent to collar membranelles. The right ciliary field comprises 26 kineties, left ciliary field comprises 21 kineties on average. The lateral ciliary field comprises 25 kineties on average, the rightmost kinety of the lateral ciliary field anterior curving rightwards and parallel to the ventral kinety. Dorsal kinety is composed of 79 dikinetids on average. Posterior kinety with about 28 dikinetids, located below the fifteenth kinety of the left ciliary field. One buccal membranelle; on average 18 collar membranelles, five of them elongated into the buccal cavity.

Neotype of *Leprotintinnus simplex*

This species was originally discovered from the Gulf of Siam, Thailand (Schmidt, 1902). No information on the holotype is available. Hence a neotype should be assigned to this species. The neotype population was sampled from the coast of Xiamen, southern China (118°6′10″E, 24°28′54″N). One protargol-stained slide (registration number: HT20201228107a) including the neotype (marked with a black circle) and four slides (registration numbers: HT20201228107b-e) with voucher

TABLE 1 | Morphometric data of *Leprotintinnus nordqvisti* (upper line) and *L. simplex* (lower line).

Characteristics	Min	Max	$\bar{x}$	M	SD	SE	CV	N
Lorica, total length	80.0	185.0	137.1	137.5	22.2	5.1	16.2	19
	170.0	425.0	253.8	227.5	67.9	15.2	26.7	20
Anterior aperture diameter	37.0	46.0	41.2	40.0	2.9	0.7	6.9	19
	57.0	68.0	63.4	63.0	3.6	0.8	5.7	20
Posterior opening diameter	28.0	45.0	34.8	35.0	4.5	1.0	12.8	19
	30.0	63.0	53.2	55.0	6.3	1.4	11.8	20
Lorica total length: anterior aperture, ratio	2.0	4.2	3.3	3.2	0.6	0.1	17.3	19
	3.0	6.5	4.0	3.7	0.9	0.2	22.9	20
Cell proper, length	33.0	95.0	61.0	60.0	14.6	2.9	23.9	25
	45.0	130.0	70.7	64.0	22.3	5.8	31.5	15
Cell proper, width	30.0	49.0	39.8	40.0	5.3	1.1	13.3	25
	47.0	65.0	53.6	53.0	4.8	1.2	9.0	15
Cell proper length:width, ratio	0.9	2.3	1.5	1.6	0.3	0.1	21.3	25
	0.8	2.0	1.3	1.3	0.3	0.1	25.7	15
Macronucleus nodules, number	1.0	3.0	2.0	2.0	0.4	0.1	20.7	30
	2.0	3.0	2.1	2.0	0.2	0.1	12.1	15
Anterior macronucleus nodule, length	7.0	20.0	14.6	15.0	3.1	0.6	21.1	25
	12.0	35.0	20.3	20.0	5.6	1.4	27.5	15
Anterior macronucleus nodule, width	7.0	20.0	12.9	12.0	3.7	0.7	28.7	25
	10.0	22.0	14.1	13.0	3.8	1.0	27.3	15
Posterior macronucleus nodule, length	10.0	26.0	16.6	16.0	3.2	0.6	19.3	25
	10.0	33.0	21.7	20.0	6.5	1.7	29.9	15
Posterior macronucleus nodule, width	7.0	17.0	11.6	11.0	2.5	0.5	21.8	25
	9.0	20.0	15.0	15.0	3.0	0.8	19.9	15
Anterior cell end to anterior macronucleus nodule, distance	6.0	17.0	10.5	11.0	2.3	0.5	21.6	25
	8.0	25.0	17.3	16.0	4.2	1.1	24.4	15
Micronuclei, number	1.0	2.0	1.1	1.0	0.3	0.1	29.4	8
	–	–	–	–	–	–	–	–
Micronucleus, diameter	2.0	2.0	2.0	2.0	0.0	0.0	0.0	8
	–	–	–	–	–	–	–	–
Ventral kinety, length	25.0	42.0	32.0	32.0	4.8	1.3	15.1	15
	32.0	65.0	47.7	51.0	12.0	3.1	25.2	15
Ventral kinety, number of kinetids	25.0	53.0	41.6	42.0	7.3	1.9	17.5	15
	48.0	84.0	67.2	64.0	11.4	2.9	17.0	15
Ventral kinety, distance to anterior end of cell	1.0	1.0	1.0	1.0	0.0	0.0	0.0	15
	1.0	1.0	1.0	1.0	0.0	0.0	0.0	15
Dorsal kinety, length	45.0	72.0	57.6	57.0	8.7	2.2	15.1	15
	56.0	141.0	83.5	73.0	23.6	6.1	28.3	15
Dorsal kinety, number of dikinetids	25.0	43.0	33.6	36.0	6.1	1.4	18.2	20
	61.0	103.0	79.1	78.0	11.7	3.0	14.8	15
Dorsal kinety, distance to right ciliary field	4.0	8.0	5.9	6.0	1.1	0.3	18.3	11
	3.0	12.0	6.5	6.0	2.9	0.9	45.2	10
Dorsal kinety, distance to left ciliary field	7.0	14.0	10.3	11.0	2.2	0.7	21.2	11
	7.0	20.0	15.4	17.5	4.6	1.5	29.9	10
Dorsal kinety, distance to collar membranelles	4.0	7.0	5.2	5.0	0.9	0.2	17.8	20
	2.0	5.0	3.5	3.0	1.0	0.3	29.5	15
Posterior kinety, length	27.0	47.0	36.2	35.0	6.3	1.9	17.5	11
	20.0	82.0	41.3	35.0	15.7	4.0	37.9	15
Posterior kinety, number of dikinetids	11.0	20.0	14.5	14.0	2.3	0.6	15.9	15
	19.0	40.0	27.7	27.0	6.0	1.5	21.6	15
Posterior kinety, distance to dorsal kinety	5.0	12.0	6.6	6.0	2.0	0.5	30.2	15
	3.0	24.0	11.5	12.0	4.6	1.2	39.9	15
Posterior kinety, distance to collar membranelles	21.0	45.0	28.9	28.0	5.8	1.5	20.1	15

(Continued)

TABLE 1 | (Continued)

Characteristics	Min	Max	$\bar{x}$	M	SD	SE	CV	N
	18.0	50.0	34.3	35.0	8.7	2.3	25.5	15
Right ciliary field, number of kineties	13.0	15.0	13.5	13.0	0.6	0.1	4.2	25
	24.0	27.0	25.6	26.0	0.8	0.2	3.3	17
Kinety 1 in right ciliary field, length	6.0	16.0	10.7	10.0	2.9	0.8	27.3	15
	10.0	21.0	14.9	15.0	3.5	0.9	23.4	15
Kinety 1 in right ciliary field, number of kinetids	4.0	11.0	6.6	6.0	2.0	0.5	29.7	15
	7.0	13.0	10.5	10.0	1.8	0.5	16.9	15
Kinety 1 in right ciliary field, distance to collar membranelles	8.0	14.0	10.7	10.0	1.8	0.5	16.8	15
	10.0	25.0	14.6	14.0	4.5	1.2	30.6	15
Kinety n in right ciliary field, length	7.0	11.0	9.2	10.0	1.5	0.5	16.6	11
	8.0	22.0	12.9	13.0	3.7	1.0	28.9	15
Kinety n in right ciliary field, number of kinetids	4.0	6.0	4.4	4.0	0.6	0.2	14.7	11
	5.0	12.0	8.2	9.0	2.1	0.6	26.0	15
Kinety n in right ciliary field, distance to collar membranelles	5.0	10.0	7.6	8.0	1.4	0.4	18.7	11
	7.0	15.0	10.2	9.0	3.1	0.8	30.8	15
Lateral ciliary field, number of kineties	16.0	19.0	17.4	17.0	0.7	0.1	4.3	25
	23.0	27.0	24.8	24.0	1.6	0.4	6.6	15
Lateral ciliary field, width	25.0	35.0	29.5	30.0	3.3	1.3	11.2	6
	30.0	42.0	36.3	37.0	4.1	1.1	11.2	15
Kinety 1 in lateral ciliary field, length	5.0	11.0	8.1	8.0	1.9	0.6	23.1	10
	11.0	20.0	15.3	15.0	2.2	0.6	14.2	15
Kinety 1 in lateral ciliary field, number of kinetids	4.0	10.0	6.5	6.5	1.7	0.6	26.9	10
	9.0	14.0	11.6	12.0	1.4	0.4	12.1	15
Kinety 1 in lateral ciliary field, distance to collar membranelles	3.0	8.0	5.7	5.5	1.3	0.4	23.6	10
	4.0	9.0	5.9	5.0	1.4	0.4	23.4	15
Kinety n -1 in lateral ciliary field, length	16.0	25.0	20.6	21.0	3.3	1.5	15.8	5
	30.0	54.0	39.4	38.0	8.2	3.7	20.8	5
Kinety n-1 in lateral ciliary field, number of kinetids	20.0	38.0	29.2	28.0	6.6	2.9	22.4	5
	42.0	58.0	49.4	48.0	5.4	2.4	10.8	5
Kinety n - 1 in lateral ciliary field, distance to collar membranelles	3.0	5.0	4.2	4.5	0.9	0.3	20.8	10
	2.0	7.0	4.6	5.0	1.9	0.8	40.3	5
Kinety n in lateral ciliary field, length	18.0	26.0	23.0	23.0	2.8	1.2	12.0	5
	28.0	59.0	46.8	48.0	10.6	4.7	22.6	5
Kinety n in lateral ciliary field, number of kinetids	24.0	46.0	32.0	30.0	7.5	3.3	23.4	5
	48.0	78.0	61.0	60.0	9.9	4.4	16.2	5
Kinety n in lateral ciliary field, distance to collar membranelles	1.0	2.0	1.2	1.0	0.4	0.2	33.3	5
	1.0	2.0	1.4	1.0	0.5	0.2	35.0	5
Left ciliary field, number of kineties	10.0	12.0	11.2	11.0	0.6	0.1	5.1	25
	18.0	22.0	20.5	21.0	1.3	0.6	6.4	15
Kinety 1 in left ciliary field, length	1.0	5.0	3.0	3.0	1.5	0.5	51.6	10
	2.0	5.0	3.0	3.0	0.8	0.4	27.2	15
Kinety 1 in left ciliary field, number of kinetids	1.0	3.0	1.6	1.5	0.7	0.2	41.5	10
	1.0	3.0	2.0	2.0	0.7	0.3	36.5	15
Kinety 1 in left ciliary field, distance to collar membranelles	5.0	7.0	6.3	6.0	0.6	0.2	10.2	10
	4.0	8.0	6.3	6.0	1.3	0.6	20.6	15
Kinety n in left ciliary field, length	7.0	12.0	9.0	8.5	2.0	0.6	22.2	10
	10.0	19.0	15.0	16.0	2.4	1.1	16.0	15
Kinety n in left ciliary field, number of kinetids	4.0	7.0	5.4	5.5	0.9	0.3	17.0	10
	5.0	12.0	9.6	10.0	1.6	0.7	16.9	15
Kinety n in left ciliary field, distance to collar membranelles	7.0	12.0	9.0	8.5	2.0	0.6	22.2	10
	3.0	8.0	5.5	5.0	1.3	0.6	22.7	15
Adoral zone of membranelles, diameter	31.0	48.0	40.9	41.0	4.4	0.9	10.9	25
	52.0	67.0	56.7	54.0	4.6	2.1	8.2	15

(Continued)

TABLE 1 | (Continued)

Characteristics	Min	Max	$\bar{x}$	M	SD	SE	CV	N
Collar membranelles, number	20.0	21.0	20.5	21.0	0.5	0.1	2.4	25
	17.0	18.0	17.8	18.0	0.4	0.2	2.2	15
Collar membranelles, number of elongated ones	4.0	4.0	4.0	4.0	0.0	0.0	0.0	25
	5.0	5.0	5.0	5.0	0.0	0.0	0.0	15
Buccal membranelle, number	1.0	1.0	1.0	1.0	0.0	0.0	0.0	25
	1.0	1.0	1.0	1.0	0.0	0.0	0.0	25

Lorica data are based on live observations, and others are based on protargol-stained specimens. Measurements in μm. Min, minimum; Max, maximum; $\bar{x}$, arithmetic mean; M, median; SD, standard deviation; SE, standard error of arithmetic mean; CV, coefficient of variation in %; N, number of specimens examined; –, Null value.

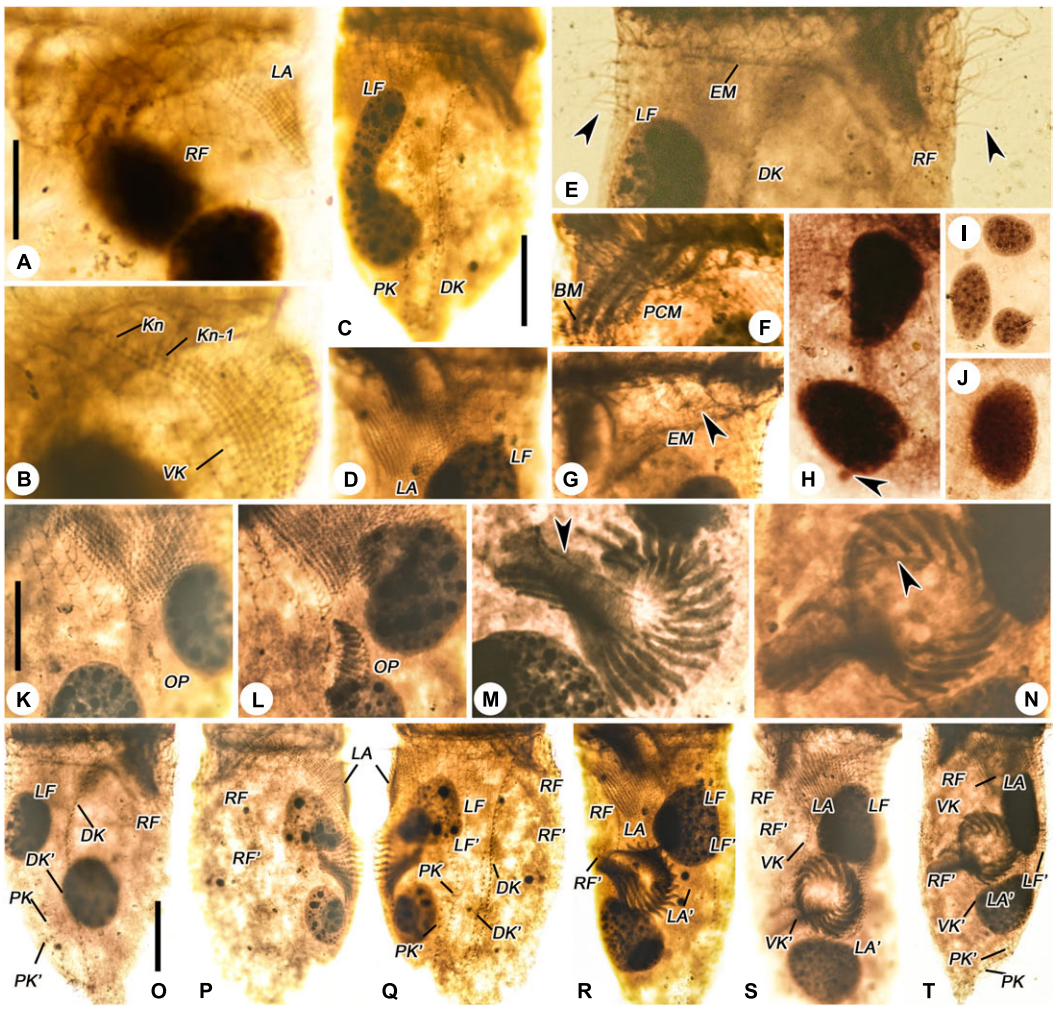

FIGURE 3 | *Leprotintinnus nordqvisti* after protargol staining. **(A,B)** Ventrolateral view showing the ventral kinety, right ciliary field, and lateral ciliary field. **(C)** Dorsal view of an anterdivider, showing left ciliary field, dorsal and posterior kineties. **(D)** Lateral ciliary field and left ciliary field. **(E)** The anterior portion of dorsal kinety, left ciliary field, and right ciliary field, arrows indicate the elongated anterior cilia of the right and left ciliary fields. **(F)** Prolonged collar membranelles and buccal membranelle. **(G)** Arrowhead shows the endoral membrane. **(H–J)** Macronuclear nodules and micronuclei (arrowhead). **(K,L)** Ventral view of early dividers. **(M,N)** Oral primordium, arrows indicate opisthe's endoral membranelle. **(O)** Dorsal view of the same very early divide. **(P,Q)** Ventral and dorsal views of the same early middle divide. **(R)** Ventral view of the middle divider. **(S)** Ventral view of the late middle divide, showing the split of the ventral kinety. **(T)** Ventral view of the middle-to-late divider. BM, buccal membranelle; DK, DK′, proter's and opisthe's dorsal kineties; EM, endoral membranelle; LA, LA′, proter's and opisthe's lateral ciliary fields; LF, LF′, proter's and opisthe's left ciliary fields; OP, oral primordium; PCM, prolonged collar membranelles; RF, RF′, proter's and opisthe's right ciliary fields; VK, VK′, proter's and opisthe's ventral kineties. Scale bars: 20 μm.

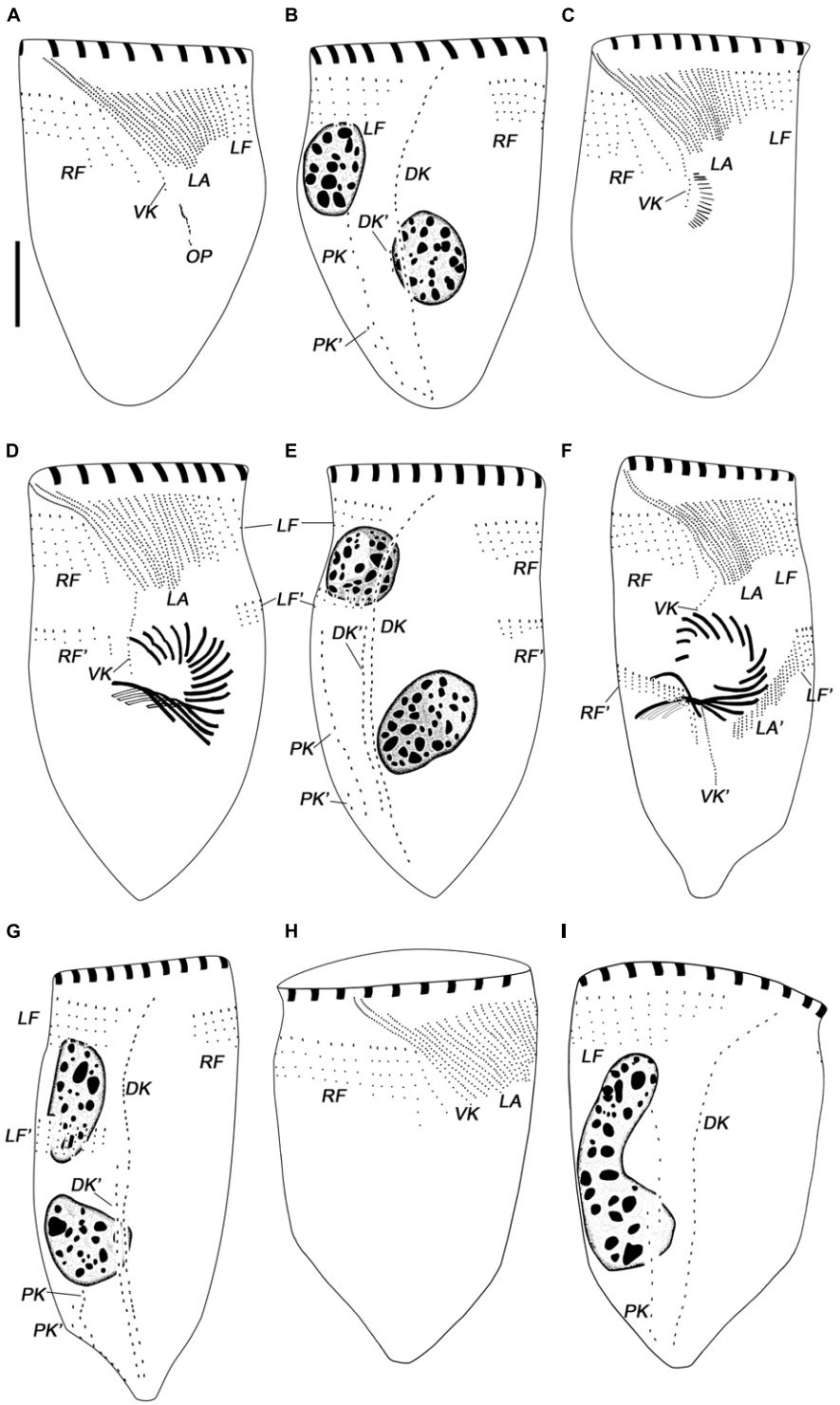

FIGURE 4 | *Leprotintinnus nordqvisti*, dividers after protargol staining. **(A,B)** Ventral and dorsal views of the same very early divider. **(C)** Ventral views of an early divider. **(D,E)** Ventral and dorsal views of the same late middle divider. **(F,G)** Ventral and dorsal views of the same middle-to-late divider. **(H,I)** Ventral and dorsal views of a new cell. DK, DK′, proter's and opisthe's dorsal kineties; LA, LA′, proter's and opisthe's lateral ciliary fields; LF, LF′, proter's and opisthe's left ciliary fields; OP, oral primordium; RF, RF′, proter's and opisthe's right ciliary fields; VK, VK′, proter's and opisthe's ventral kineties. Scale bars: 20 μm.

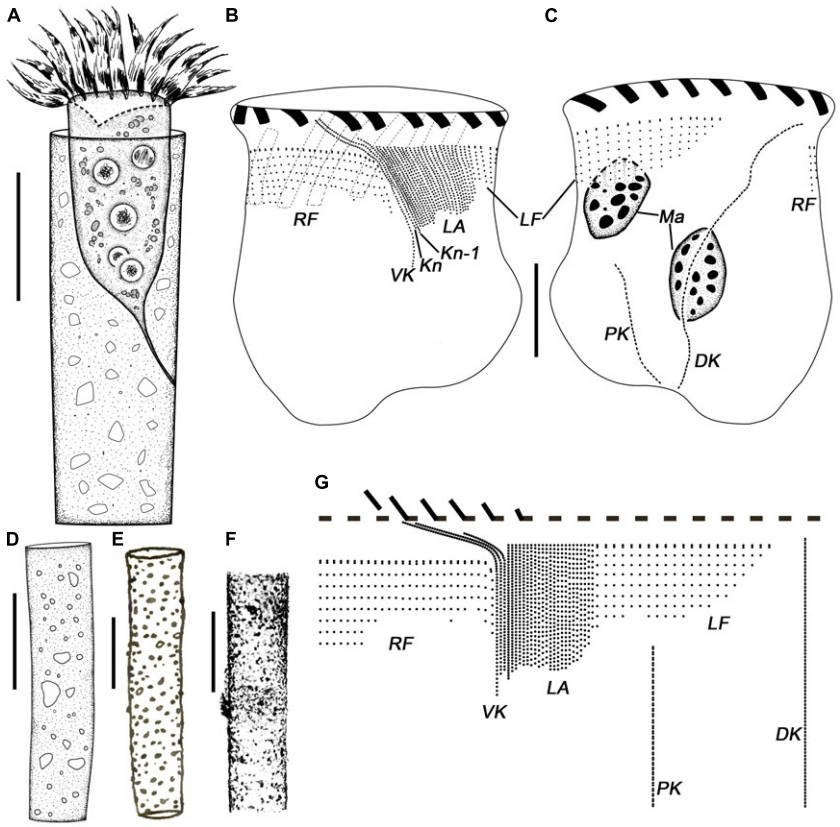

FIGURE 5 | *Leprotintinnus simplex* from life **(A,D–F)** and after protargol staining **(B,C,G)**. **(A)** Lateral view of a typical individual. **(B,C)** The ciliary pattern of ventral and dorsal sides of the same specimen. **(D)** Loricae with agglomerated mineral particles. **(E)** Lateral view of loricae from Schmidt, 1902. **(F)** *L. neriticus* from Yoo et al., 1988. **(G)** Kinetal map of a morphostatic specimen. DK, dorsal kinety; K_n, the last kinety of the lateral ciliary field; K_{n-1}, the penultimate kinety of the lateral ciliary field; LA, lateral ciliary field; LF, left ciliary field; Ma, macronuclear nodules; RF, right ciliary field; VK, ventral kinety. Scale bars: 40 μm **(A,D–F)**, 20 μm **(B,C)**.

specimens were deposited in the Laboratory of Protozoology, Ocean University of China, Qingdao, China.

Morphological Description of *Leprotintinnus simplex*

Lorica cylindrical, about 170–425 μm, gradually tapering (2°–4°) to the aboral end, and slightly curved in some individuals (**Figures 5A,D**, **6A–G** and **Table 1**). Aperture 57–68 μm in diameter without an oral flare (**Figures 5A,D**, **6A–E**). The ratio of length to opening diameter is 2.6–6.5:1. The aboral margin is often ragged, without a flare or a constriction, about 30–63 μm across (**Figures 5A,D**, **6A–E**). Wall comparatively thin, sparsely agglutinated with particles, about 2–10 × 2–13 μm in size (**Figures 5D**, **6G**).

Naked live cells elongate doliform, usually 42–50 × 40–55 μm in size (**Figures 5A**, **6F** and **Table 1**). After protargol staining, specimens about 45–130 × 47–65 μm in size. Two, rarely three, ellipsoidal macronuclear nodules centrally located in the cytoplasm, each about 10–35 × 9–22 μm in size, with nucleoli about 2 μm across, anterior nodule 8–25 μm posteriorly to the anterior cell end (**Figures 5C**, **6H–J** and **Table 1**). Micronuclei not recognized. Neither striae, tentaculoids, accessory combs, contractile vacuole, cytopyge, nor capsule was observed. Cytoplasm colorless and granular, with food vacuoles up to 5 μm across containing yellow microalgae (**Figure 6F**). Slow swimming motion while rotating the main body cell axis. When picked and dropped onto clean glass slides *in vivo*, cells tend to escape from the loricae.

The somatic ciliary pattern of the most complex type (Agatha and Strüder-Kypke, 2007), i.e., comprising a ventral, a dorsal, and a posterior kinety as well as a right, a left, and a lateral ciliary field (**Figures 5B,C,G**, **6H–M** and **Table 1**). Kinetids of each ciliary row ostensibly connected by argyrophilic fibers (**Figures 6H–M**). Ventral kinety about 32–65 μm long, commencing about 1 μm below the anterior end of the cell, anterior to the twelfth or thirteenth kinety of the right ciliary field, rarely anterior to the eighth or ninth one. Ventral kinety curving leftwards and extending parallel to kineties of the lateral ciliary field, and then terminated at the postmedian of cell proper, consisting of 48–84 ciliated monokinetids, which are closely spaced anterior but widely spaced posteriorly, cilium about 2 μm long after impregnation (**Figures 5B,G**, **6H,J,L**). The right ciliary field commences about 7–15 μm posteriorly to the collar membranelles except for the first kinety (the leftmost

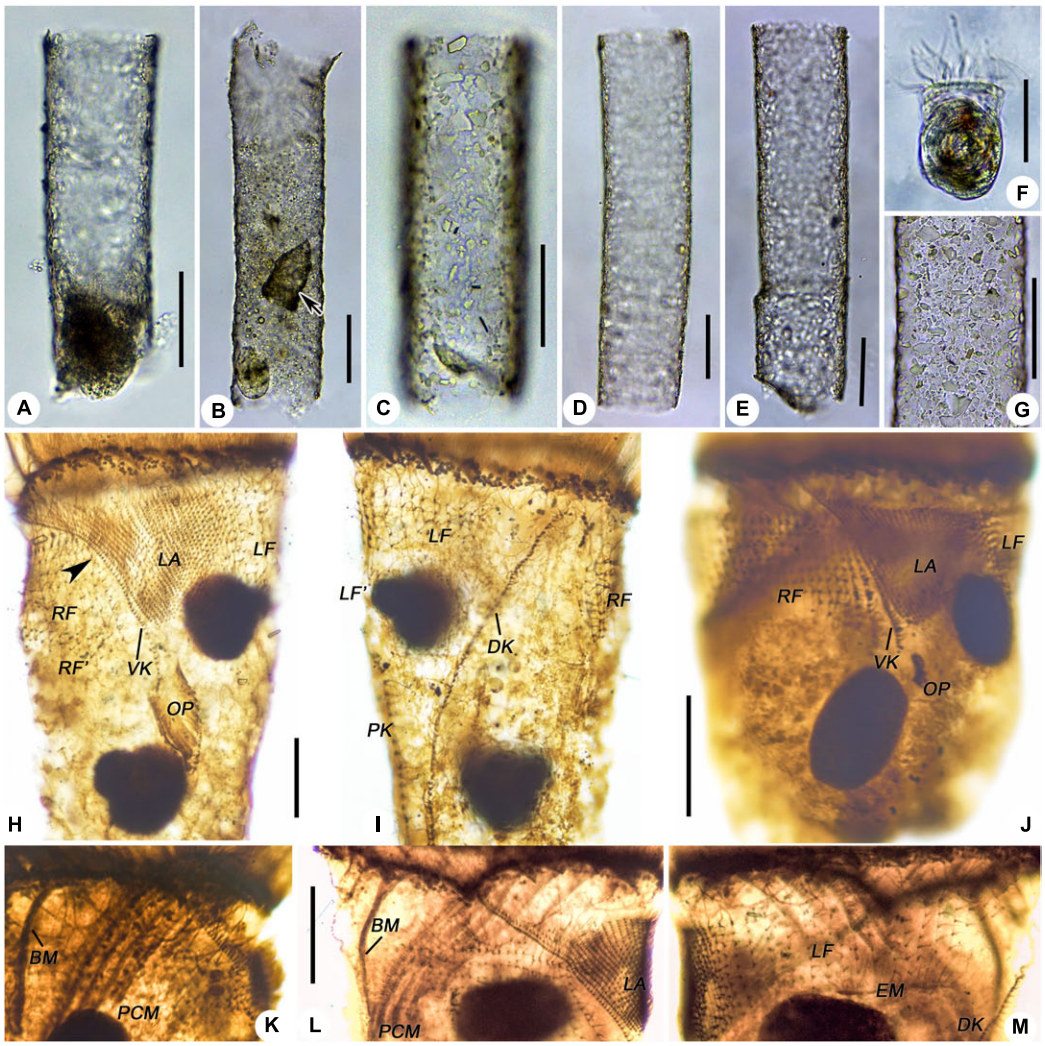

FIGURE 6 | *Leprotintinnus simplex* from life **(A–G)** and after protargol staining **(H–M)**. **(A)** A representative specimen. **(B–E)** Showing the variability of loricae shape and size, the arrow denotes a predated *Tintinnopsis* sp. **(F)** Cell proper out of the lorica. **(G)** Lorica wall with numerous mineral particles. **(H,I)** Ventral and dorsal views of the same specimen, showing the ciliary pattern, arrowhead indicates the dikinetids at the anterior end of the right ciliary field. **(J)** Ventral view of an early divider, showing the location of the oral primordium and the posterior end of the VK. **(K)** Prolonged membranelles and buccal membranelle. **(L)** Lateral view showing the right ciliary filed and the anterior position of the VK; M, Left ciliary field, dorsal kinety, and endoral membranelle. BM, buccal membranelle; DK, dorsal kinety; EM, endoral membranelle; LA, lateral ciliary field; LF, LF′, proter's and opisthe's left ciliary fields; OP, oral primordium; PCM, prolonged collar membranelles; RF, RF′, proter's and opisthe's right ciliary field; VK, ventral kinety. Scale bars: 50 μm **(A–G)**, 15 μm **(H–M)**.

one), which commences about 10–25 μm posterior to the collar membranelles. The kinety of the right ciliary field comprising 24–27 kineties, about 8–22 μm long, with a space about 2 μm, consisting of 4–12 monokinetids and one dikinetid anterior, the first kinety with two anterior dikinetids in a few specimens (**Figures 5B,C,G**, **6H–J,L**). Cilia of the right ciliary field about 4–5 μm long after protargol impregnation and the anterior cilium of each dikinetids about 15–18 μm (**Figures 6H–J,L**). Dorsal kinety about 56–141 μm long, commencing about 2–5 μm posterior to collar membranelles, about 7–20 μm apart from the left ciliary fields, and about 3–12 μm apart from the right ciliary fields, curving to the left and extending to the posterior end of cell proper, consisting of 61–103 dikinetids, with a cilium about 10–13 μm long (after protargol impregnation) on each posterior basal body (**Figures 5C,G**, **6I,M**). The left ciliary field commencing about 3–8 μm posterior to collar membranelles, comprising 18–22 kineties, about 2–19 μm long, with a space about 2–3 μm, consisting of 1–12 monokinetids and one anterior dikinetid, the first kinety often comprising of only one anterior dikinetid (**Figures 5B,C,G**, **6H,I,M**). Cilia of the left ciliary field about 10 μm long after protargol impregnation, and the anterior cilium of each dikinetids about 18 μm (**Figures 6H,I,M**). The lateral ciliary field commencing about 4–9 μm posteriorly to collar membranelles, except for (i) the last kinety (K_n) commencing close to the anterior end of the ventral kinety and extending parallel to the ventral kinety,

and (ii) the penultimate kinety (K_{n-1}) commencing about 2–7 μm posterior to collar membranelles, anterior to the fifth or sixth kinety of the right ciliary field, lower than the anterior end of K_n and higher than that of other kineties. The lateral ciliary field comprising 23–27 kineties, each kinety consisting of 9–14 densely spaced monokinetids about 11–20 μm long, excluding K_n and K_{n-1} which consist of 48–78 (28–59 μm long) and 42–58 (30–54 μm long) densely spaced monokinetids, respectively. The monokinetid with a space about 1 μm; cilia about 6-μm long after protargol impregnation (**Figures 5B,G**, **6H,J,L**). Posterior kinety about 20–82 μm long, commencing about 13–35 μm posterior to the fifteenth (occasionally the thirteenth) kinety of the left ciliary field (about 18–50 μm posterior to collar membranelles), and about 3–24 μm apart from the dorsal kinety, and extending almost longitudinally to the posterior end of cell proper, consisting of 19–40 dikinetids, with a cilium about 5–9 μm long (after protargol impregnation) on each posterior basal body (**Figures 5C,G**, **6I**).

Oral apparatus forming a closed circle at anterior cell end, 52–67 μm across after protargol staining, consisting of 17–18 collar membranelles and invariably one buccal membranelle (**Figures 5B,C,G**, **6K** and **Table 1**). Collar membranelles up to 23–55 μm long, separated by shallow ridges about 20 μm wide, consisting of three rows of basal bodies, with cilia up to about 20–30 μm long (**Figures 5B**, **6K**). Polykinetids of the proximal-most five collar membranelles successively elongated, extending into the 30–35 μm deep buccal cavity (**Figures 5B**, **6K**). Single buccal membranelle, with a base about 30–38 μm long (**Figures 5B**, **6K**). Endoral membrane extending across the peristomial field and right side of the buccal cavity, composed of a single row of ciliated monokinetids (**Figures 5B**, **6K**). Argyrophilic fibers were barely recognizable.

Ontogenesis of *Leprotintinnus simplex*

Only several individuals in cell division were stained. *L. simplex* shows an enantiotropic division mode as observed in several early and middle dividers. The hypoapokinetal somitogenesis occurred in a subsurface pouch located on the left of ventral kinety and posteriorly to the lateral ciliary field (**Figures 6H–J**).

Sequences Comparison and Phylogenetic Analyses

For the two species investigated, three nuclear rDNA markers (18S, ITS1-5.8S-ITS2, and 28S genes) and one mitochondrial marker (*CO1* gene) were sequenced. The sequences length, G+C content, and GenBank accession numbers are shown in **Table 2**. Each of three rDNA sequences of *L. nordqvisti* in different aboral forms (with or without an aboral flare) were completely identical, respectively. Intraspecific genetic variations among individuals in the *CO1* gene were 1.43% (7 nucleotide difference) and version 0.2% (1 nt) for *L. nordqvisti* and *L. simplex*, respectively. After removing the primers, the 18S rDNA sequences of *L. nordqvisti* newly obtained in this work differed by only one nucleotide (base deletion) from that of another population (KU715761) collected from the Jiaozhou Bay of Qingdao, China; however, its ITS1-5.8S rDNA-ITS2 (KU715800) was identical with that of our population (Zhang et al., 2017). As for *L. simplex*, the ITS1-5.8S-ITS2 and partial 28S rDNA sequences are available in the GenBank from a Jiaozhou Bay population. Sequence (KU715801) containing ITS1-5.8S-ITS2 and partial 28S rDNA is identical to the new sequence of *L. simplex* in this study. The sequence (KU715781) containing ITS2 and partial 28S rDNA differs from our population in the ITS2 region by one nucleotide (Zhang et al., 2017).

For each of these four markers, the topologies of both ML and BI trees are similar. So only the ML tree is shown. In the 18S rDNA tree, *L. nordqvisti* clusters with *Tintinnopsis radix* (KU715774, EU399540), and then form a full support clade with *L. simplex*. *Tintinnopsis lobiancoi* (JN831813), *T. pseudocylindrica* (JN831853), *Stylicauda platensis* (JN831832), *Rhizodomus tagatzi* (KU715762), *Climacocylis scalaroides* (KY290330), and *C. scalaria* (JQ408210) cluster together and form a sister group of *Leprotintinnus-Tintinnopsis* clade with nearly full support (99% ML, 1 BI) (**Figure 7**). The topologies of the ITS and 28S rDNA trees are roughly consistent with that of 18S rDNA-based analysis (**Figures 7–9**). *L. simplex* clusters with *L. nordqvisti* and *T. radix* (KU715816) clade with full support in the ITS rDNA tree (**Figure 8**). In the 28S rDNA tree, *L. nordqvisti* and *L. simplex* clade is sister to the group of *Rhizodomus tagatzi* (KU715783), *Tintinnopsis pseudocylindrica* (KU831938), and *Stylicauda platensis* (JN831918) (**Figure 9**). In the *CO1* tree, two sequences of *L. nordqvisti* cluster together, and then form a sister clade to the two sequences of *L. simplex* with weak support (56/0.98) (**Figure 10**).

DISCUSSION

Comparison of *Leprotintinnus nordqvisti* With Other Populations

Leprotintinnus nordqvisti was discovered for the first time from the Brazilian coast by Brandt (1906, 1907) named *Tintinnus nordqvisti* and then transferred to the genus *Leprotintinnus* by Kofoid and Campbell (1929) based on its lorica open at both ends. In the original report, this species was recorded as having an inverted funnel-shaped aboral flare, loricae length 105–200 μm, opening diameter 30–45 μm, and posterior opening 40–60 μm across (Brandt, 1906). Our population corresponds well with the original description, except for a slightly smaller posterior opening (28–45 μm vs. 40–60 μm) which might be caused by the absence of an aboral flare in some individuals of our population. In previous studies, the funnel-shaped aboral flare was regarded as the unique character for this species (Kofoid and Campbell, 1929). We found individuals with or without aboral flare in the same sample. In order to identify them, we extracted their DNA and performed the protargol impregnation separately for each individual with different lorica forms. The results combining both gene sequence (18S, ITS1-5.8S-ITS2, and 28S genes) and ciliary pattern verify that these individuals with or without the aboral flare are the same species. So, the identification of our population is solid. This study reveals the polymorphic loricae of *L. nordqvisti* for the first time.

TABLE 2 | Gene sequences obtained in this study.

Species (isolate type)	Marker	Length (bp)	GC content (%)	Accession number
Leprotintinnus nordqvisti (without an aboral flare)	18S rDNA	1724	47.39	OM131555
	ITS1-5.8S rDNA-ITS2	526	47.15	
	Partial 28S rDNA	805	53.04	
Leprotintinnus nordqvisti (without an aboral flare)	18S rDNA	1724	47.26	OM131556
	ITS1-5.8S rDNA-ITS2	526	47.15	
	28S rDNA	1755	50.31	
	CO1	478	39.75	OM201658
Leprotintinnus nordqvisti (with an aboral flare)	18S rDNA	1729	47.54	OM131557
	ITS1-5.8S rDNA-ITS2	526	47.15	
	Partial 28S rDNA	776	52.96	
	CO1	478	39.54	OM201659
Leprotintinnus simplex	18S rDNA	1710	47.49	OM131558
	ITS1-5.8S rDNA-ITS2	526	47.34	
	Partial 28S rDNA	759	51.91	
	CO1	478	41.21	OM201660
Leprotintinnus simplex	*CO1*	478	41.42	OM201661

It is interesting that Sassi et al. (2004) reported a population of *L. nordqvisti* from neritic waters of Northeast Brazil and recorded that some loricae without the typical aboral dilatation common or with the dilatation little evident. Its loricae characters are in agreement with those of our population, i.e., lorica length (72.9–295.8 μm vs. 80–185 μm), anterior opening diameter (31.2–43.7 μm vs. 37–46 μm), and posterior opening across (23.2–122.9 μm vs. 28–45 μm). Our work confirms the speculation of Sassi et al. (2004).

Roxas (1941) also reported a population of tintinnids from the coast of Manila Bay and found some of the individuals with aboral flare but others without. Roxas (1941) identified the specimens with basal portion well expanded as *L. nordqvisti* (lorica length 118 μm, opening diameter 40 μm, posterior opening 78 μm) and those aboral end unexpanded as a new species, *L. tubulosus* Roxas (1941) (lorica length 140 μm, opening diameter 37 μm). In terms of loricae shape and size, *L. tubulosus* is identical to the specimens of *L. nordqvisti* without an aboral flare in our study. Therefore, *L. tubulosus* Roxas (1941) might be a synonym of *L. nordqvisti*.

The lorica with an aboral flare is unique to *L. nordqvisti* and can be easily distinguished from other tintinnids. This species had been reported many times in different seas (**Table 3**). The loricae length and opening diameters of these populations roughly coincide with those of our study, except for variations at the posterior flared portion.

Comparison of *Leprotintinnus nordqvisti* With Related Species

The typical lorica with a conspicuous funnel-shaped aboral flare makes *L. nordqvisti* to be distinguished easily from its congeners. Given that the aboral flare is now no longer a stable feature of *L. nordqvisti*, however, four similar congeners should be compared with *L. nordqvisti*, namely *L. elongatus* Skryabin and Al-Yamani, 2007, *L. bubiyanicus* Skryabin and Al-Yamani, 2007, *L. neriticus* (Campbell, 1926) Kofoid and Campbell, 1929, and *L. simplex* Schmidt, 1902.

Leprotintinnus elongatus is very similar with *L. nordqvisti* in lorica shape (tube-like lorica with slightly flaring oral and aboral ends vs. oral margin slightly flared and posterior end little widened in some individuals) and size of opening diameter (32.5–42.5 μm vs. 37–46 μm) (Skryabin and Al-Yamani, 2007). The loricae length of *L. elongatus* is significantly longer than that of *L. nordqvisti* (212.5–332.5 μm vs. 80–185 μm), the measurement of its loricae length, however, likely included whole loricae with epilorica according to the illustrations given by Skryabin and Al-Yamani (2007). This implies that its actual length excluding epilorica would overlap with the range of *L. nordqvisti* in this study. In addition, according to Skryabin and Al-Yamani (2007), *L. elongatus* differed from *L. nordqvisti* by the absence of the aboral funnel. However, our study revealed the polymorphic loricae of *L. nordqvisti*, namely its aboral funnel might be absent in some individuals. So, *L. elongatus* and *L. nordqvisti* cannot be discriminated against by the aboral funnel. Therefore, *L. elongatus* is very likely to be a synonym of *L. nordqvisti*. Their relationship is pending further information on cytological and molecular data of *L. elongatus*.

Leprotintinnus nordqvisti differs from *L. bubiyanicus* and *L. neriticus* by its smaller opening diameter (37–46 μm in the former vs. 72.1–82.4 μm in *L. bubiyanicus*, vs. 120–175 μm in *L. neriticus*; Campbell, 1926; Skryabin and Al-Yamani, 2007). *Leprotintinnus nordqvisti* can be separated from *L. simplex* by the lorica shape (oral end flaring vs. never flaring), size (80–185 μm vs.170–425 μm in length, and 37–46 μm vs. 57.5–67.5 μm in opening diameter), and ciliary patterns (see below) (Schmidt, 1902).

Occurrence and Ecology of *Leprotintinnus nordqvisti*

The compilation is limited to *L. nordqvisti* and its synonym suggested above (see **Table 3**). Note that only some of them were substantiated by morphometric data and/or illustrations, therefore, misidentification cannot be excluded.

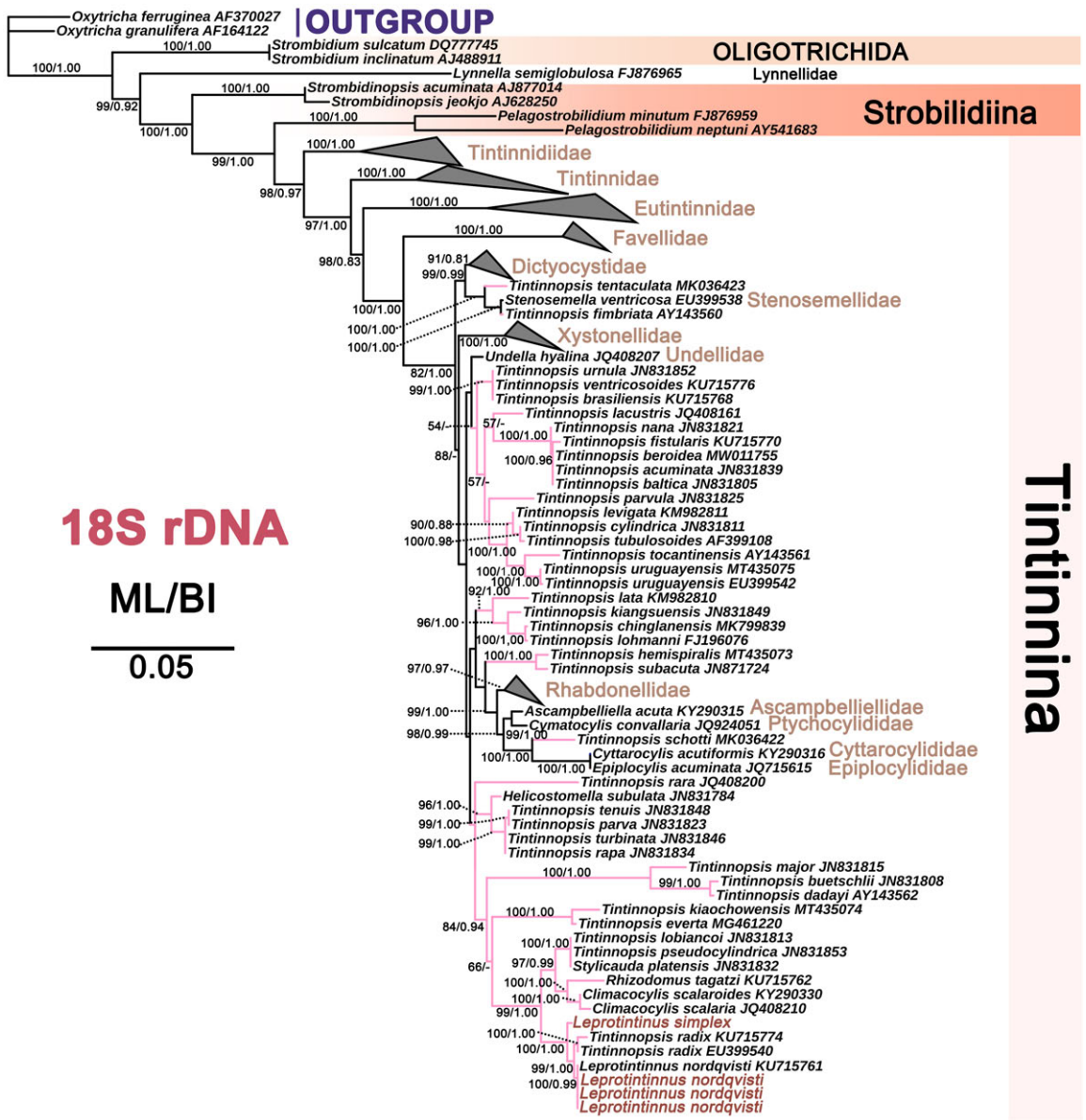

FIGURE 7 | The maximum likelihood (ML) phylogenetic tree is inferred from 18S rDNA sequences. Numbers at the nodes represent support values in the following order: ML and BI bootstrap values. The pink branch denotes the incertae sedis taxa in Tintinnina. The new sequences *Leprotintinnus nericus* and *L. simplex* in the present work were indicated in red. A hyphen (–) represents support values too low (ML < 45%, BI < 0.70) and disagreements in topology between the BI and ML trees. The scale bar corresponds to 5 substitutions per 100 nucleotides.

According to Hada (1974), the species was found at a water temperature of about 29.1–29.5°C, a salinity of about 28.38–33.26‰, and a pH of about 7.9–8, which were basically closed to the environmental factors in our study (salinity 27‰, pH 8.1, and water temperature 23.5°C). In Li et al. (2019), *L. nordqvisti* was considered as a brackish species, occurring at a salinity range of 9.2–34.1‰. During winter and early spring, the abundance of *L. nordqvisti* was higher in Kuwait waters (Yousif Al-Yamani et al., 2011). A 10-year (May 2003 to December 2012) survey in Jiaozhou Bay, however, found that the species occurs in April, May, and July to October with a maximum abundance of 130 ind/L (Feng et al., 2018). Wang et al. (2014) recorded an abundance of.73 ± 0.54 ind/L and biomass of 12.68 ± 9.75 ng C/L in the Northern Beibu Gulf, the South China Sea in August 2011.

Comparison of *Leprotintinnus simplex* With Other Populations

Leprotintinnus simplex originally found from the Gulf of Siam was recorded with a lorica 204 μm long and the anterior opening 41 μm across (Schmidt, 1902). Although the aboral diameter was not provided in the original description, it can be inferred

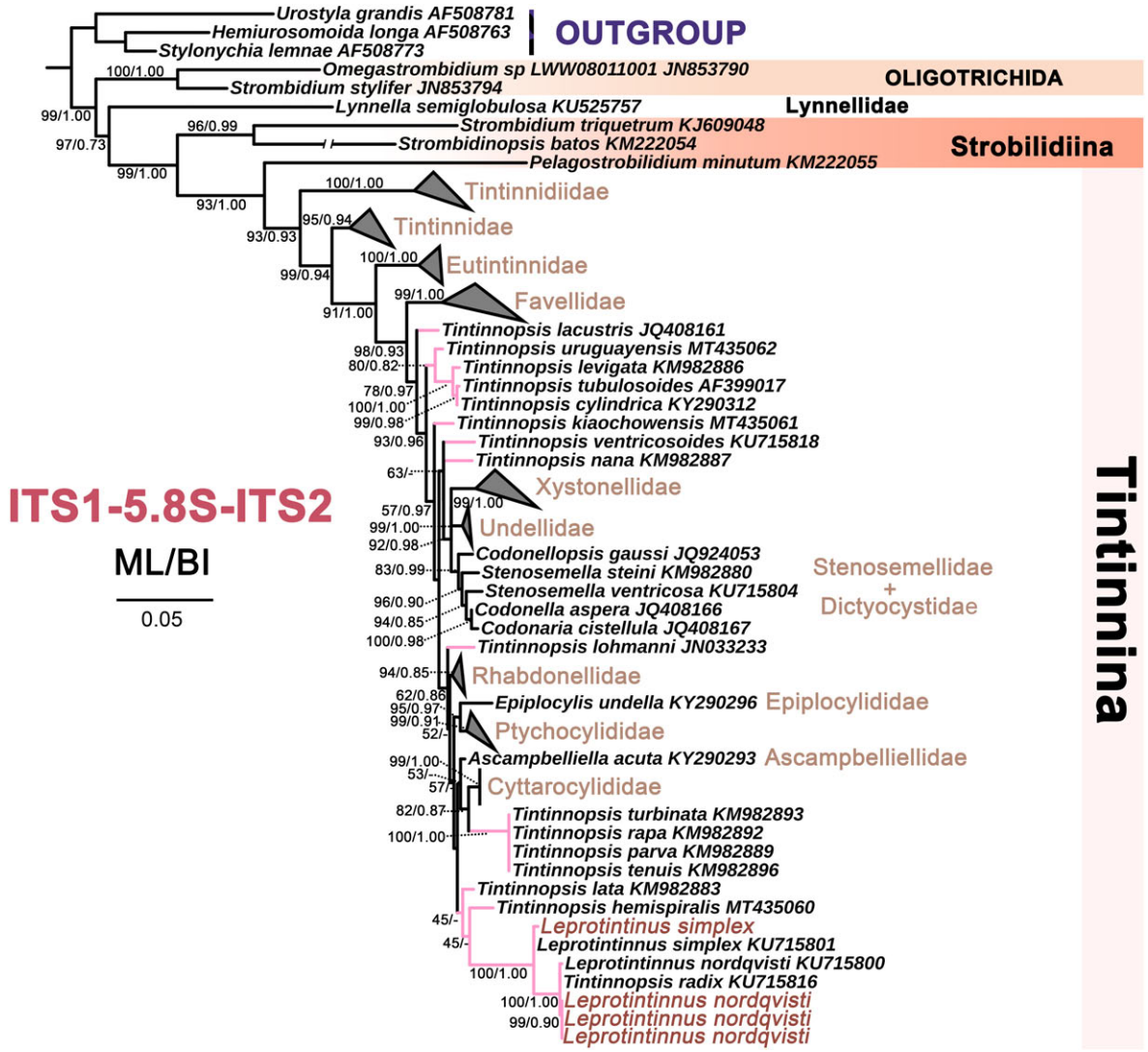

FIGURE 8 | The maximum likelihood (ML) phylogenetic tree is inferred from ITS1-5.8S rDNA-ITS2 sequences. Numbers at the nodes represent support values in the following order: ML and BI bootstrap values. The pink branch denotes the incertae sedis taxa in Tintinnina. The new sequences *Leprotintinnus nerititicus* and *L. simplex* in the present work were indicated in red. A hyphen (–) represents support values too low (ML < 45%, BI < 0.70) and disagreements in topology between the BI and ML trees. The scale bar corresponds to 5 substitutions per 100 nucleotides.

from the single illustration as about 35 μm. Our population corresponds well with the original description in terms of lorica shape (cylindrical or subcylindrical lorica) and length (170–425 μm vs. 204 μm), although there are slight differences in the opening diameter of the anterior end (57–68 μm vs. 41 μm) and the aboral end (30–63 μm vs. about 35 μm), which might be caused by different amount of loricae that measured or the difference among populations. So, our population was finally identified as *L. simplex* Schmidt (1902). This identification was supported by the population of Zhang et al. (2017), which was reported having similar lorica length (175 μm vs. 170–425 μm) with our population and similar opening diameter (42 μm vs. 41 μm) with the original population. What's more, the population of Zhang et al. (2017) had almost identical ITS and partial 28S rDNA sequences with those of our population. So, Zhang et al. (2017) help to confirm our species identification.

The study of Yoo et al. (1988) described a tintinnid species, *Leprotintinnus nerititicus* in Chinhae Bay in November 1981. Its lorica characters are significantly different from the original description of this species, i.e., lorica length (320–430 μm vs. 380–470 μm), opening diameter (60 μm vs. 120–175 μm), aboral diameter (50–55 μm vs. 90–172 μm) (Campbell, 1926). However, the population of Yoo et al. (1988) matches perfectly with our population in terms of the lorica shape (simple, tubular lorica vs. cylindrical lorica), length (320–430 μm vs. 170–425 μm), opening diameter (60 μm vs. 57–68 μm), and aboral diameter (50–55 μm vs. 30–63 μm). It is noteworthy that, in Yoo et al. (1988), a population of *L. simplex* with lorica length

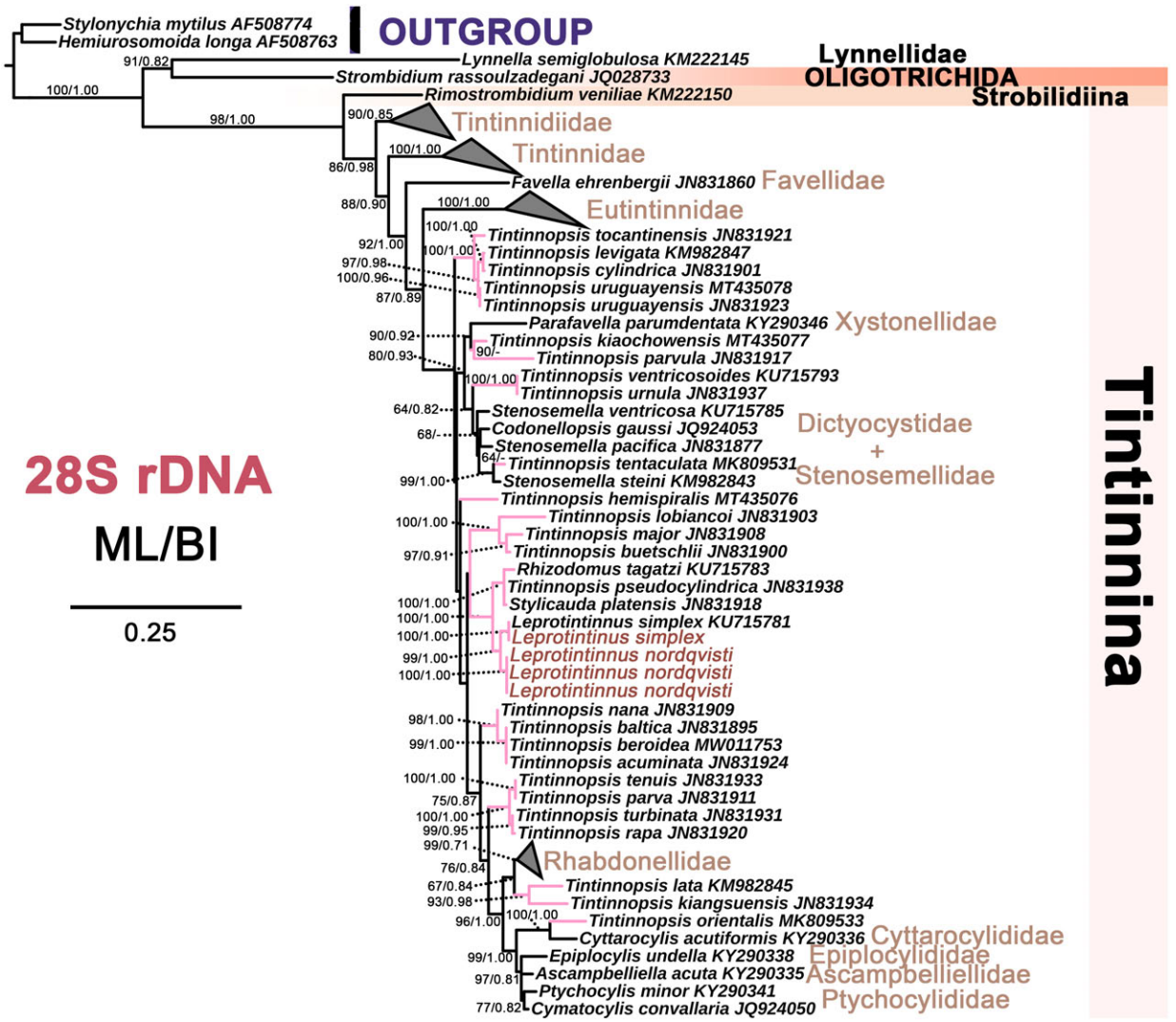

FIGURE 9 | The maximum likelihood (ML) phylogenetic tree is inferred from 28S rDNA sequences. Numbers at the nodes represent support values in the following order: ML and BI bootstrap values. The pink branch denotes the incertae sedis taxa in Tintinnina. The new sequences *Leprotintinnus nericus* and *L. simplex* in the present work were indicated in red. A hyphen (–) represents support values too low (ML < 45%, BI < 0.70) and disagreements in topology between the BI and ML trees. The scale bar corresponds to 25 substitutions per 100 nucleotides.

200 μm and opening diameter of 38 μm was also found from the same site with its *L. neriticus* population. Therefore, *L. neriticus* sensu Yoo et al. (1988) might be a misidentification of *L. simplex*.

Leprotintinnus simplex had also been recorded from western tropical Pacific with lorica length 205 μm and opening diameter of 38 μm (Hada, 1938), coastal waters of Qingdao with lorica length 250–360 μm and opening diameter 50–60 μm (Xu and Song, 2005), Chilika Lagoon with lorica length 297.32 μm and opening diameter 58.19 μm (Mukherjee et al., 2015), Jiaozhou Bay, China with lorica length 175 μm and opening diameter 42 μm (Zhang et al., 2017), and coastal waters of Xiamen with lorica length 340–415 μm and opening diameter 61–67 μm (Liao et al., 2018). The loricae length and opening diameters of all above populations roughly coincide with our population (lorica length 170–425 μm, opening diameter 57–68 μm) and original description (lorica 204 μm long and the anterior opening 41 μm across) of *L. simplex* (**Table 3**).

Comparison of *Leprotintinnus simplex* With Related Species

The four *Leprotintinnus* species are similar to *L. simplex* by their cylindrical or subcylindrical lorica without sharp narrowing of the aboral end, namely *L. nordqvisti* (Brandt, 1906) Kofoid and Campbell, 1929, *L. bubiyanicus* Skryabin and Al-Yamani, 2007, *L. elongatus* Skryabin and Al-Yamani, 2007, and *L. neriticus* (Campbell, 1926) Kofoid and Campbell, 1929. *L. simplex* can be distinguished out by its smaller anterior opening (57–68 μm) from *L. bubiyanicus* (vs. 72.1–82.4 μm) and *L. neriticus* (vs. 120–175 μm) (Campbell, 1926; Skryabin and Al-Yamani, 2007).

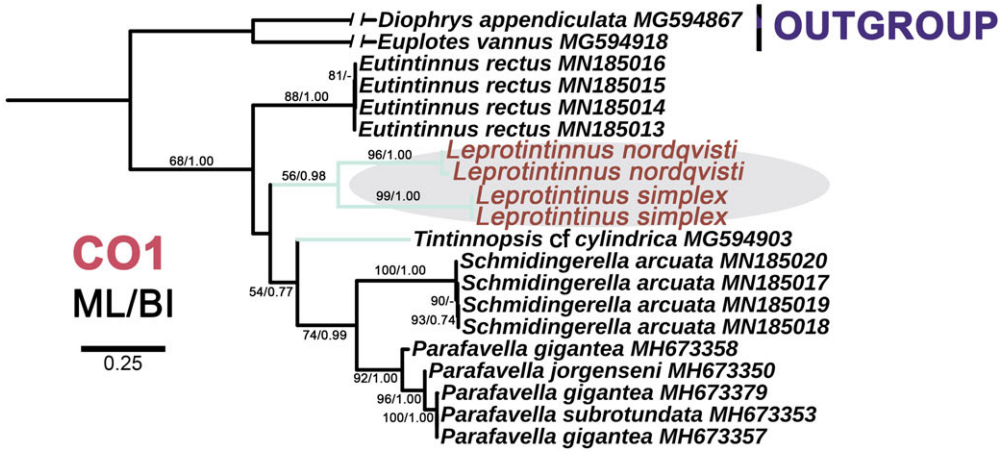

FIGURE 10 | The maximum likelihood (ML) phylogenetic tree is inferred from *CO1* gene sequences. Numbers at the nodes represent support values in the following order: ML and BI bootstrap values. The green branch denotes the incertae sedis taxa in Tintinnina. The new sequences *Leprotintinnus nerititicus* and *L. simplex* in the present work were indicated in red. A hyphen (–) represents support values too low (ML < 45%, BI < 0.70) and disagreements in topology between the BI and ML trees. The scale bar corresponds to 25 substitutions per 100 nucleotides.

L. simplex differs from *L. elongatus* by the absence of the flaring oral end (Skryabin and Al-Yamani, 2007).

Leprotintinnus nordqvisti and *L. simplex* are the only two species with known ciliary patterns in the genus at present. Both species have very similar cell features, but can be distinguished from each other by the starting position of the ventral kinety (anteriorly to the fifth or sixth kinety of the right ciliary field in the former vs. to the twelfth or thirteenth kinety of the right ciliary field) and kinety numbers of the right (13–15 vs. 24–27), left (10–12 vs. 18–22), and lateral (16–19 vs. 23–27) ciliary field.

Occurrence and Ecology of *Leprotintinnus simplex*

The compilation is limited to *L. simplex* populations (see **Table 3**). Note that only some of them were substantiated by morphometric data and/or illustrations, therefore, misidentification cannot be excluded.

In the study of Li et al. (2019), *L. simplex* was considered as a brackish species, occurring at a salinity range of 11.8–34.1‰. A 10-year (May 2003 to December 2012) survey in Jiaozhou Bay, found that the species excluding May were present with a maximum abundance of 130 ind/L (Feng et al., 2018). In August 2011, Wang et al. (2014) recorded an abundance of 20.63 ± 11.09 ind/L and biomass of 161.60 ± 74.14 ng C/L in the Northern Beibu Gulf, South China Sea.

Ontogenesis of *Leprotintinnus* in Tintinnids

The cell division of *Leprotintinnus* matches that previously reported species with a complex somatic ciliary pattern in the position of the oral primordium (e.g., Petz and Foissner, 1993; Laval-Peuto, 1994; Agatha and Riedel-Lorjé, 2006; Agatha and Tsai, 2008; Gruber et al., 2018). In these reports, it appears that the dorsal and posterior kineties of the daughter cells are broken from old (parental) structures, as the right side of the old structures does not develop basal body proliferation. However, only in *Tintinnopsis everta* was reported a late middle divider showing the splits of dorsal and posterior kineties, which differs from the *de novo* proliferation that we reported in the present study. Unfortunately, we failed to observe the separation of dorsal and posterior kineties in the very late stages of ontogenesis. We speculate that the kineties position of the opisthe is asymmetrical to the proter due to the breakage of the argyrophilic fibers in the very late stages of cell division, with the left ciliary field of the opisthe closer to the right than that in the proter. Through this gap, the posterior and dorsal kineties of the proter gradually move upwards as the cell body extends and rotates, while the posterior and dorsal kineties of the opisthe gradually move downwards. Finally, the proter and opisthe separate, acquiring the old and new structures, respectively.

The Ciliary Pattern of *Leprotintinnus* in Tintinnids

This study reveals that the ciliary pattern of the genus *Leprotintinnus* is attributed to the most complex type, which consists of a ventral, a dorsal, and a posterior kinety as well as a right, a left, and a lateral ciliary field (Agatha and Strüder-Kypke, 2007). This type of ciliary pattern has been reported in many other genera, such as *Codonlla* (affiliation doubtful) (Foissner et al., 1999), *Codonellopsis* (Petz et al., 1995; Kim et al., 2013), *Laackmanniella* (Kim et al., 2013), *Cymatocylis* (Wasik and Mikolajczyk, 1994; Petz et al., 1995), *Stenosemella* (Agatha and Tsai, 2008), *Tintinnopsis* (Gruber et al., 2018), and *Schmidingerella* (Agatha and Strüder-Kypke, 2012). The differences in the ciliary patterns of these species are very slight, except for the position of the posterior kinety is shifty. At present, it is still difficult to distinguish different families or genera by this type of ciliary pattern. We can only help future taxonomic revise by reporting more cell features that reveal new patterns of

TABLE 3 | Morphology and distribution of reported populations of *Leprotintinnus nordqvisti* and *L. simplex*.

Species	Location	Lorica length (μm)	Anterior aperture diameter (μm)	Posterior opening diameter (μm)	Ref.
L. nordqvisti	Coast of Brazilian	105–200	30–45	40–60	Brandt, 1906
	Bay of Amoy	200	about six times the oral diameter in length	–	Wang and Nie, 1932
	Tropical Pacific	150–352	30–38	40–80	Hada, 1938
	Coast of Manila Bay	118	40	78	Roxas, 1941
L. tubulosus (original name)	Coast of Manila Bay	140	37	–	Roxas, 1941
	Gulf of California	144	43	66	Osorio-Tafall, 1941
	Arabian Sea Coast of India	125–270	37–43	30–33	Hada, 1974
	Chinhae Bay	135–240	33–38	48–83	Yoo et al., 1988
	Uranouchi Inlet	108–223	33–44	56–95	Nakamachi and Iwasaki, 1998
	Subtropical waters of the Southern Brazil	154–215	38–39	45–75	Fernandes, 2004
	Coast of Brazilian	72.9–295.8	31.2–43.7	23.2–122.9	Sassi et al., 2004
	Kuwait Waters	128–192	43 ± 1	109–154	Yousif Al-Yamani et al., 2011
	Coastal waters off Guangdong	200	40	80	Zhang et al., 2012
	The Northern Beibu Gulf	–	–	–	Wang et al., 2014
	Chilika Lagoon	180	41.71	83.87	Mukherjee et al., 2015
	Jiaozhou Bay	156	45	–	Zhang et al., 2017
	Coast of Manila Bay	182–243	36–49	–	Santiago et al., 2017
	The coastal zone of India	–	–	–	Elangovan and Gauns, 2018
	Jiaozhou Bay	–	–	–	Feng et al., 2018
	The Pearl River Estuary in southern China	–	–	–	Li et al., 2019
	The North Western Coast of the Red Sea	–	–	–	Saber et al., 2021
	An oyster farm of Yanjiang	80–185	37–46	28–45	Present work
L. simplex	Gulf of Siam	204	41	–	Schmidt, 1902
	Western tropical Pacific	205	38	–	Hada, 1938
	Hiroshima Bay	–	–	–	
	Chinhae Bay	200	38	–	Yoo et al., 1988
Original name *L. neriticus*	Chinhae Bay	320–430	60	50–55	Yoo et al., 1988
	Coastal waters off Qingdao	250–360	50–60	–	Xu and Song, 2005
	The Northern Beibu Gulf	–	–	–	Wang et al., 2014
	Chilika Lagoon	297.32	58.19	–	Mukherjee et al., 2015
	Jiaozhou Bay	175	42	–	Zhang et al., 2017
	The coastal zone of India	–	–	–	Elangovan and Gauns, 2018
	Jiaozhou Bay	–	–	–	Feng et al., 2018
	Coastal waters off Amoy	340–415	61–67	–	Liao et al., 2018
	The Pearl River Estuary in southern China	–	–	–	Li et al., 2019
	Yundang Lake of Amoy	170–425	57–68	30–63	Present work

–, Null value.

somatic ciliature or some subtle but very important features in the most complex ciliature pattern (Agatha and Strüder-Kypke, 2012; Gruber et al., 2018).

Tintinnopsis radix (Imhof, 1886) Brandt, 1907 and *Rhizodomus tagatzi* Strelkow and Wirketis, 1950 are the most similar tintinnid species to *L. nordqvisti* and *L. simplex* based on their common ciliary pattern, i.e., the ventral kinety curving drastically to the right and extending anterior to the right ciliary field, and the posterior kinety positioned below the left ciliary field (Jiang et al., 2012; Saccà et al., 2012). These four species can be distinguished by each other by the complexity of different numbers of kineties. In addition, *L. nordqvisti* and *L. simplex* can be distinguished from *T. radix* and *R. tagatzi* by the position of the anterior end of the rightmost two lateral kineties. It should not be omitted that *R. tagatzi* in Saccà et al. (2012), the dorsal kinety of it composed of monokinetids, which is significantly different from *Leprotintinnus*. Naturally, without electron microscopic studies, it cannot be excluded that the dorsal kinety consists indeed of dikinetids with only one basal body ciliated and that the unciliated basal body was not recognized due to insufficient staining.

Bai et al. (2020) reported *Tintinnopsis* cf. *radix* with a very similar ciliary pattern to *Leprotintinnus*, namely both the ventral kinety and the rightmost two lateral kineties largely curved above the kinety of the right ciliary field from photomicrographs. However, the posterior kinety of the former commences below the ventral kinety (vs. below the left ciliary field for *Leprotintinnus*). The taxonomic significance of the position of the posterior kinety at the genus or family level is still unclear. Bai et al. (2020) did not provide any molecular data of *Tintinnopsis* cf. *radix*. Therefore, its relationship with *Leprotintinnus* is pending.

Leprotintinnus nordqvisti and *L. simplex* are also similar with *Tintinnopsis everta* in the significant anterior extending of the ventral kinety and the last lateral kinety, however, the latter can be separated from them by the position of the anterior end of the ventral and the rightmost two lateral kineties (see below). Gruber et al. (2018) had assumed that the evolution of the ventral kinety might gradually be curving rightward, extending anterior to the kinety of the right ciliary field, simultaneously with a parallel extension of the last kinety of the lateral ciliary field. Considering that the anterior end of the ventral and the rightmost two lateral kineties in *L. nordqvisti* and *L. simplex* extending further than that of *T. everta*, *L. nordqvisti,* and *L. simplex* may provide a later stage than *T. everta* in the evolution of the ventral kinety reconstruction.

Phylogeny of *Leprotintinnus* in Tintinnids

Our phylogeny analyses show that *Leprotintinnus* species cluster with *Tintinnopsis radix* with full support, and then form a big clade with some species of *Tintinnopsis*, *Stylicauda*, *Rhizodomus*, and *Climacocylis* with nearly full support. This result is consistent with some previous reports (Santoferrara et al., 2017). In terms of loricae features, the genera *Tintinnopsis*, *Leprotintinnus*, *Rhizodomus*, and *Stylicauda* differ from *Climacocylis* by having the sparsely agglutinated loricae (vs. hyaline loricae in *Climacocylis*). This is apparently inconsistent with the phylogenetic relationship shown in the molecular trees. Therefore, all these genera were assigned to *incertae sedis* in Tintinnina (Santoferrara et al., 2017; Zhang et al., 2017). The species with available ciliary patterns in this phylogeny clade, i.e., *L. nordqvisti, L. simplex, T. radix*, and *R. tagatzi* display high similarities in terms of their cytological features (Saccà et al., 2012). This agrees with the phylogeny results and suggests their homologous evolution in morphology. However, considering that most ciliary patterns in this clade have not been revealed yet, the taxonomic data are still not enough to revise the classification of the species contained in this branch. Nevertheless, we can speculate that the large anterior extending of the ventral kinety together with the last or penultimate lateral kinety is likely to be a promising distinguishing feature of this clade or genus of *Leprotintinnus*. Also, given that most of the loricae in this clade are sparse agglutination, they likely represent a homology in the wall ultrastructure or lorica matrix material (Agatha and Bartel, 2021).

DATA AVAILABILITY STATEMENT

The datasets presented in this study can be found in online repositories. The names of the repository/repositories and accession number(s) can be found below: NCBI [accession: OM131555-OM131558 and OM201658-OM201661].

AUTHOR CONTRIBUTIONS

XL conceived and directed the research. TH and ZW performed the sampling and conducted the taxonomic and phylogenetic work. TH and WL identified the species. TH drafted the manuscript. ZW, WL, and XL made further revisions. All authors approved the submitted version of manuscript.

FUNDING

This work was supported by the projects of the National Natural Science Foundation of China (42076113 and 31761133001) and the Fundamental Research Funds for the Central Universities (20720200106).

ACKNOWLEDGMENTS

Many thanks are due to Sabine Agatha for her kindly helping to provide important literature Campbell (1926).

REFERENCES

Adl, S. M., Bass, D., Lane, C. E., Lukes, J., Schoch, C. L., Smirnov, A., et al. (2019). Revisions to the classification, nomenclature, and diversity of Eukaryotes. *J. Eukaryot. Microbiol.* 66, 4–119. doi: 10.1111/jeu.12691

Agatha, S., and Bartel, H. (2021). A comparative ultrastructural study of tintinnid loricae (Alveolata, Ciliophora, Spirotricha) and a hypothesis on their evolution. *J. Eukaryot. Microbiol.* Online ahead of print. doi: 10.1111/jeu.12877

Agatha, S., and Riedel-Lorjé, J. C. (2006). Redescription of Tintinnopsis cylindrica Daday, 1887 (Ciliophora : Spirotricha) and unification of tintinnid terminology. *Acta Protozool.* 45, 137–151.

Agatha, S., and Strüder-Kypke, M. C. (2007). Phylogeny of the order Choreotrichida (Ciliophora, Spirotricha, Oligotrichea) as inferred from morphology, ultrastructure, ontogenesis, and SSrRNA gene sequences. *Eur. J. Protistol.* 43, 37–63. doi: 10.1016/j.ejop.2006.10.001

Agatha, S., and Strüder-Kypke, M. C. (2012). Reconciling cladistic and genetic analyses in *Choreotrichid ciliates* (Ciliophora, Spirotricha, Oligotrichea). *J. Eukaryot. Microbiol.* 59, 325–350. doi: 10.1111/j.1550-7408.2012.00623.x

Agatha, S., and Tsai, S.-F. (2008). Redescription of the tintinnid Stenosemella pacifica Kofoid and Campbell, 1929 (Ciliophora, Spirotricha) based on live observation, protargol impregnation, and scanning electron microscopy. *J. Eukaryot. Microbiol.* 55, 75–85. doi: 10.1111/j.1550-7408.2008.00309.x

Bai, Y., Wang, R., Song, W., Suzuki, T., and Hu, X. Z. (2020). Redescription of five tintinnine ciliates (Alveolata: Ciliophora: Oligotrichea) from coastal waters of Qingdao. *China. Mar. Life Sci. Technol.* 2, 209–221. doi: 10.1007/s42995-020-00034-32

Brandt, K. A. H. (1906). *Die Tintinnodeen der Plankton-Expedition. Tafelerklarungen Nebst Kurzer Diagnose der Neuen Arten*. Kiel: Lipsius & Tischer.

Brandt, K. A. H. (1907). "Die tintinnodeen der plankton-expedition. systematischer teil," in *Ergebnisse der Plankton-Expedition der Humboldt-Stiftung 3 La*, ed. V. Hensen (Kiel: Lepsius and Tischer).

Campbell, A. S. (1926). On *Tintinnus neriticus* sp. nov., from San Francisco bay. *Univ. Calif. Publ. Zool.* 29, 237–239.

Cleve, P. T. (1899). Plankton collected by the Swedish expedition to Spitzbergen in 1898. *Kongl. Sven. Vetensk. Akad. Handl.* 32, 1–51.

Corliss, J. O. (2003). Comments on the neotypification of protists, especially ciliates (Protozoa, Ciliophora). *Bull. Zool. Nom.* 60, 48–48.

Dolan, J. R. (2016). Planktonic protists: little bugs pose big problems for biodiversity assessments. *J. Plankton Res.* 38, 1044–1051. doi: 10.1093/plankt/fbv079

Dolan, J. R., Montagnes, D. J., Agatha, S., Coats, D. W., and Stoecker, D. K. (2013). *The Biology and Ecology of Tintinnid Ciliates: Models for Marine Plankton*. Wiley-Blackwell: Oxford.

Elangovan, S. S., and Gauns, M. (2018). A checklist of tintinnids (loricate ciliates) from the coastal zone of India. *Environ. Monit. Assess.* 190, 1–18. doi: 10.1007/s10661-018-7039-y

Feng, M., Wang, C., Zhang, W., Zhang, G., Xu, H., Zhao, Y., et al. (2018). Annual variation of species richness and lorica oral diameter characteristics of tintinnids in a semi-enclosed bay of western Pacific. *Estuar. Coast. Shelf S.* 207, 164–174. doi: 10.1016/j.dib.2018.06.010

Fernandes, L. F. (2004). Tintinnids (Ciliophora, Tintinnina) from subtropical waters of the Southern Brazil. I. families codonellidae, codonellopsidae, coxliellidae, cyttarocylidae, epiplocylidae, petalotrichidae, ptychocylidae, tintinnididae and undellidae. *Rev. Bras. Zool.* 21, 551–576. doi: 10.1590/s0101-81752004000300019

Foissner, W. (2002). Neotypification of protists, especially ciliates (Protozoa, Ciliophora) Wilhelm Foissner. *Bull. Zool. Nom.* 59:165.

Foissner, W., and O'Donoghue, P. J. (1990). Morphology and infraciliature of some freshwater ciliates (Protozoa: Ciliophora) from Western and South Australia. *Invertebr. Syst.* 3, 661–696. doi: 10.1071/it9890661

Foissner, W., Berger, H., and Schaumburg, J. (1999). *Identification and Ecology of Limnetic Plankton Ciliates*. München: Bartels & Wemitz.

Gold, K., and Morales, E. A. (1974). Effects of temperature on 2 strains of Tintinnopsis tubulosa. *J. Protozool.* 21, 442–442.

Gold, K., and Morales, E. A. (1975). Tintinnida of the New York Bight: loricae of *Parafavella gigantea*, *P. parumdentata*, and *Ptychocylis obtusa*. *Trans. Am. Microsc. Soc.* 94, 142–145.

Gruber, M. S., Strüder-Kypke, M., and Agatha, S. (2018). Redescription of Tintinnopsis everta Kofoid and Campbell, 1929 (Alveolata, Ciliophora, Tintinnina) based on taxonomic and genetic analyses-discovery of a new complex ciliary pattern. *J. Eukaryot. Microbiol.* 65, 484–504. doi: 10.1111/jeu.12496

Hada, Y. (1938). Studies on the Tintinnoinea from the Western Tropical Pacific (with 3 tables and 100 textfigures). *J. Fac. Sci., Hokkaido Univ. Ser.* 6, 87–190.

Hada, Y. (1974). The protozoan plankton collected from the port of Cochin on the Arabian Sea coast of India. *Univ. Liter.* 15, 73–97.

Imhof, O. E. (1886). Über microscopische pelagische Thiere aus den Lagunen von Venedig. *Zool. Anz.* 9, 101–104.

International Code of Zoological Nomenclature [ICZN] (1999). *International Code of Zoological Nomenclature: International Commission on Zoological Nomenclature*. London: London International Trust for Zoological Nomenclature.

Jerome, C. A., Lynn, D. H., and Simon, E. M. (1996). Description of *Tetrahymena empidokyrea* n. sp., a new species in the Tetrahymena pyriformis sibling species complex (Ciliophora, Oligohymenophorea), and an assessment of its phylogenetic position using small-subunit rRNA sequences. *Can. J. Zool.* 74, 1898–1906.

Ji, D. D., and Wang, Y. F. (2018). An optimized protocol of protargol staining for ciliated protozoa. *J. Eukaryot. Microbiol.* 65, 705–708. doi: 10.1111/jeu.12515

Jiang, Y., Yang, J. P., Al-Farraj, S. A., Warren, A., and Lin, X. F. (2012). Redescriptions of three tintinnid ciliates, *Tintinnopsis tocantinensis*, *T. radix, and T. cylindrica* (ciliophora, spirotrichea), from coastal waters off China. *Eur. J. Protistol.* 48, 314–325. doi: 10.1016/j.ejop.2012.02.001

Jörgensen, E. (1900). Ueber die Tintinnodeen der norwegischen Westktüste. *Bergens Museums Aarbog.* 1899, 1–48.

Jörgensen, E. (1901). Protistenplankton aus dem Nordmeere in den Jahren 1897–1900. *Bergens Mus. Aarbog 1900* 1–37. doi: 10.1515/9783112383629-003

Kalyaanamoorthy, S., Minh, B. Q., Wong, T. K., von Haeseler, A., and Jermiin, L. S. (2017). ModelFinder: fast model selection for accurate phylogenetic estimates. *Nat. Methods* 14, 587–589. doi: 10.1038/nmeth.4285

Katoh, K., and Standley, D. M. (2013). MAFFT multiple sequence alignment software version 7: improvements in performance and usability. *Mol. Biol. Evol.* 30, 772–780. doi: 10.1093/molbev/mst010

Kim, S. Y., Choi, J. K., Dolan, J. R., Shin, H. C., Lee, S., and Yang, E. J. (2013). Morphological and ribosomal DNA-based characterization of six Antarctic ciliate morphospecies from the Amundsen Sea with phylogenetic analyses. *J. Eukaryot. Microbiol.* 60, 497–513. doi: 10.1111/jeu.12057

Kofoid, C. A., and Campbell, A. S. (1929). A conspectus of the marine and freshwater Ciliata belonging to the suborder Tintinnoinea, with descriptions of new species principally from the Agassiz Expedition to the eastern tropical Pacific, 1904-1905. *Univ. Calif. Publ. Zool.* 34, 1–403.

Kofoid, C. A., and Campbell, A. S. (1939). The Ciliata: the Tintinnoinea. reports on the scientific results of the expedition to the eastern tropical Pacific, 1904-1905. *Bull. Museum Comparative Zool. Harvard* 84, 1–473.

Kumar, S., Stecher, G., and Tamura, K. (2016). MEGA7: molecular evolutionary genetics analysis version 7.0 *for bigger datasets*. *Mol. Biol. Evol.* 33, 1870–1874. doi: 10.1093/molbev/msw054

Laval-Peuto, M. (1977). Reconstruction d'une lorica de forme Coxliella par le trophonte nu de *Favella ehrenbergii* (Ciliata, Tintinnina). *Comptes Rendus Hebdomadaires Seances l'Academie Sci. Paris Série D* 284, 547–550.

Laval-Peuto, M. (1981). Construction of the lorica in ciliata Tintinnina. in vivo study of *Favella ehrenbergii*: variability of the phenotypes during the cycle, biology, statistics, biometry. *Protistologica* 17, 249–272.

Laval-Peuto, M. (1994). Classe des Oligotrichea Bütschli, 1887. *Ordre des Tintinnida Kofoid et Campbell,* 1929. Traité de Zoologie. Anatomie, systématique, biologie. II. *Infusoires Ciliés* 2, 181–219.

Li, H., Wang, C., Liang, C., Zhao, Y., Zhang, W., Grégori, G., et al. (2019). Diversity and distribution of tintinnid ciliates along salinity gradient in the Pearl River Estuary in southern China. *Estuar. Coast. Shelf S.* 226:106268. doi: 10.1016/j.ecss.2019.106268

Liao, Y. Y., Liu, Z. Y., He, R. Y., Jiao, N. Z., and Xu, D. P. (2018). Tindinnid ciliates (protozoa, ciliophora) from coastal waters off Xiamen. *Acta Hydrobiol. Sin.* 42, 1027–1036.

Liu, W. W., Shin, M. K., Yi, Z. Z., and Tan, Y. H. (2020). Progress in studies on the diversity and distribution of planktonic ciliates (Protista, Ciliophora) in the South China Sea. *Mar. Life Sci. Technol.* 3, 28–43. doi: 10.1007/s42995-020-00070-y

Medlin, L., Elwood, H. J., Stickel, S., and Sogin, M. L. (1988). The characterization of enzymatically amplified eukaryotic 16S-like rRNA-coding regions. *Gene* 71, 491–499. doi: 10.1016/0378-1119(88)90066-2

Minh, B. Q., Nguyen, M. A. T., and von Haeseler, A. (2013). Ultrafast approximation for phylogenetic bootstrap. *Mol. Biol. Evol.* 30, 1188–1195. doi: 10.1093/molbev/mst024

Moreira, D., von, der Heyden, S., Bass, D., López-García, P., Chao, E., et al. (2007). Global eukaryote phylogeny: combined small-and large-subunit ribosomal DNA trees support monophyly of Rhizaria, Retaria and Excavata. *Mol. Phylogenet. Evol.* 44, 255–266. doi: 10.1016/j.ympev.2006.11.001

Mukherjee, M., Banik, S. K., Pradhan, S. K., Sharma, A. P., Suresh, V., Manna, R. K., et al. (2015). Diversity and distribution of tintinnids in Chilika Lagoon with description of new records. *Indian J. Fish.* 62, 25–32.

Müller, O. F. (1776). *Zoologiae Danicae Prodromus, seu Animalium Daniae et Norvegiae Indigenarum Characteres, Nomina, et Synonyma Imprimis Popularium*. Hallageriis: Havniae.

Nakamachi, M., and Iwasaki, N. (1998). List of tintinnids (Protozoa: Ciliata) in Uranouchi Inlet, Kochi, Japan. *Bull. Mar. Sci. Fish. Kochi Univ.* 18, 65–76.

Nguyen, L.-T., Schmidt, H. A., Von Haeseler, A., and Minh, B. Q. (2015). IQ-TREE: a fast and effective stochastic algorithm for estimating maximum-likelihood phylogenies. *Mol. Biol. Evol.* 32, 268–274. doi: 10.1093/molbev/msu300

Osorio-Tafall, B. F. (1941). Tintinnidos nuevos o poco conocidos del plancton neritico de México. *Revta Soc. Mex. Hist. Nat.* 2, 147–173.

Pan, X. M., Bourland, W. A., and Song, W. B. (2013). Protargol synthesis: an in-house protocol. *J. Eukaryot. Microbiol.* 60, 609–614. doi: 10.1111/jeu.12067

Park, M.-H., Jung, J.-H., Jo, E., Park, K.-M., Baek, Y.-S., Kim, S.-J., et al. (2018). Utility of mitochondrial CO1 sequences for species discrimination of Spirotrichea ciliates (Protozoa, Ciliophora). *Mitochondrial DNA A* 30, 148–155. doi: 10.1080/24701394.2018.1464563

Petz, W., and Foissner, W. (1993). Morphogenesis in some freshwater Tintinnids (Ciliophora, Oligotrichida). *Eur. J. Protistol.* 29, 106–120. doi: 10.1016/S0932-4739(11)80303-80302

Petz, W., Song, W., and Wilbert, N. (1995). *Taxonomy and Ecology of the Ciliate Fauna (Protozoa, Ciliophora) in the Endopagial and Pelagial of the Weddell Sea, Antarctica*. Land Oberösterreich: OÖ Landesmuseum.

Ronquist, F., Teslenko, M., Van Der Mark, P., Ayres, D. L., Darling, A., Höhna, S., et al. (2012). MrBayes 3.2: efficient Bayesian phylogenetic inference and model choice across a large model space. *Syst. Biol.* 61, 539–542. doi: 10.1093/sysbio/sys029

Roxas, H. A. (1941). Marine protozoa of the Philippines. *Philipp. J. Sci.* 74, 91–139.

Saber, G. A., Madkour, F. F., Hassan, M. I., and Abu El-Regal, M. A. (2021). An updated checklist of tintinnids (Order: Choreotrichida) in the north western coast of the Red Sea at Hurghada. *Alfarama J. Basic Appl. Sci.* 2, 297–306. doi: 10.21608/ajbas.2021.77616.1054

Saccà, A., Strüder-Kypke, M. C., and Lynn, D. H. (2012). Redescription of Rhizodomus tagatzi (Ciliophora: Spirotrichea: Tintinnida), based on morphology and small subunit ribosomal RNA gene sequence. *J. Eukaryot. Microbiol.* 59, 218–231. doi: 10.1111/j.1550-7408.2012.00615.x

Santiago, J. A. M., Furio, E. F., Borja, V. M., Gatdula, N. C., and Santos, M. D. (2017). "First records of tintinnid (Protozoa: Ciliophora: Tintinnina) Species in Manila Bay," in *DLSU Research Congress 2017*, ed. C. C. Salibay (Manila: De La Salle University).

Santoferrara, L. F., Alder, V. V., and McManus, G. B. (2017). Phylogeny, classification and diversity of Choreotrichia and Oligotrichia (Ciliophora, Spirotrichea). *Mol. Phylogenet. Evol.* 112, 12–22. doi: 10.1016/j.ympev.2017.03.010

Santoferrara, L. F., and McManus, G. B. (2021). "Diversity and biogeography as revealed by morphologies and DNA sequences: Tintinnid ciliates as an example," in *Zooplankton Ecology*, 1st Edn, eds M. A. Teodósio and A. B. Barbosa (Boca Raton, FL: CRC Press), 85–118. doi: 10.1201/9781351021821-7

Santoferrara, L. F., Bachy, C., Alder, V. A., Gong, J., Kim, Y. O., Sacca, A., et al. (2016). Updating biodiversity studies in loricate protists: the case of the tintinnids (Alveolata, Ciliophora, Spirotrichea). *J. Eukaryot. Microbiol.* 63, 651–656. doi: 10.1111/jeu.12303

Santoferrara, L. F., McManus, G. B., and Alder, V. A. (2013). Utility of genetic markers and morphology for species discrimination within the order Tintinnida (Ciliophora, Spirotrichea). *Protist* 164, 24–36. doi: 10.1016/j.protis.2011.12.002

Santoferrara, L. F., Tian, M., Alder, V. A., and McManus, G. B. (2015). Discrimination of closely related species in tintinnid ciliates: new insights on crypticity and polymorphism in the genus Helicostomella. *Protist* 166, 78–92. doi: 10.1016/j.protis.2014.11.005

Sassi, R., Lima, M. F. D., Galvão, T. C. D. O., and Costa, C. F. (2004). Tintinnina (Potozoa: Ciliophora: Oligotrichida) de águas costeras do nordeste do Brasil. *Arquivos Ciências Mar.* 37, 15–27.

Schmidt, J. (1902). Some tintinnodea from the Gulf of Siam. *Vidensk. Meddel. Naturh. Kjøbenhavn* 1901, 183–190.

Skryabin, V. A., and Al-Yamani, F. Y. (2007). New species of genera Leprotintinnus and Luminella (Ciliophora, Spirotrichea, Tintinnida) from Kuwait's waters of the Arabian Gulf. *Kuwait J. Sci. Eng.* 34:79.

Smith, S. A., Song, W., Gavrilova, N. A., Kurilov, A. V., Liu, W., McManus, G. B., et al. (2018). *Dartintinnus alderae* n. g., n. sp., a brackish water tintinnid (Ciliophora, Spirotrichea) with dual-ended lorica collapsibility. *J. Eukaryot. Microbiol.* 65, 400–411. doi: 10.1111/jeu.12485

Sniezek, J. H., Capriulo, G. M., Small, E. B., and Russo, A. (1991). *Nolaclusilis hudsonicus* n. sp. (Nolaclusiliidae n. fam.) a bilaterally symmetrical tintinnine ciliate from the lower Hudson River estuary. *J. Protozool.* 38, 589–594.

Snyder, R. A., and Brownlee, D. C. (1991). *Nolaclusilis bicornis* n. g., n. sp. (Tintinnina Tintinnidiidae): a tintinnine ciliate with novel lorica and cell morphology from the Chesapeake Bay estuary. *J. Protozool.* 38, 583–589.

Sonnenberg, R., Nolte, A. W., and Tautz, D. (2007). An evaluation of LSU rDNA D1-D2 sequences for their use in species identification. *Front. Zool.* 4:6. doi: 10.1186/1742-9994-4-6

Strelkow, A. A., and Wirketis, M. A. (1950). New planktonic infusorian (suborder Tintinnoinea) from Peter the Great Bay. *Rep. USSR Acad. Sci.* 74, 389–391.

Talavera, G., and Castresana, J. (2007). Improvement of phylogenies after removing divergent and ambiguously aligned blocks from protein sequence alignments. *Syst. Biol.* 56, 564–577. doi: 10.1080/10635150701472164

Wang, C. C., and Nie, D. (1932). A survey of the marine protozoa of Amoy. *Contr. Biol. Sci. Soc. China* 8, 283–385.

Wang, Y., Zhang, W., Lin, Y., Cao, W., Zheng, L., and Yang, J. (2014). Phosphorus, nitrogen and chlorophyll-a are significant factors controlling ciliate communities in summer in the northern Beibu Gulf, South China Sea. *PLoS One* 9:e101121. doi: 10.1371/journal.pone.0101121

Wasik, A., and Mikolajczyk, E. (1994). Infraciliature of Cymatocylis affinis/convallaria (Tintinnina). *Acta Protozool.* 33, 79–85.

Xu, D. P., and Song, W. B. (2005). Tintinnid ciliates from Qingdao (Protozoa, Ciliophora, Tintinnida). *Acta Zool. Sin.* 30, 501–508.

Xu, D. P., Sun, P., Shin, M. K., and Kim, Y. O. (2012). Species boundaries in tintinnid ciliates: a case study–morphometric variability, molecular characterization, and temporal distribution of Helicostomella species (Ciliophora, Tintinnina). *J. Eukaryot. Microbiol.* 59, 351–358. doi: 10.1111/j.1550-7408.2012.00625.x

Yoo, K., Kim, Y.-O., and Kim, D.-Y. (1988). Taxonomical studies on tintinnids (Protozoa: Ciliata) in Korean coastal waters. 1. Chinhae Bay. *Bull. Korean Fish. Soc.* 4, 67–90.

Yousif Al-Yamani, F., Skryabin, V., Gubanova, A., Khvorov, S., and Prusova, I. (2011). *Marine Zooplankton Practical Guide for the Northwestern Arabian Gulf*. Kuwait: Kuwait Institute for Scientific Research.

Zhang, Q. Q., Agatha, S., Zhang, W. C., Dong, J., Yu, Y., Jiao, N. Z., et al. (2017). Three rDNA loci-Based phylogenies of tintinnid ciliates (Ciliophora, Spirotrichea, Choreotrichida). *J. Eukaryot. Microbiol.* 64, 226–241. doi: 10.1111/jeu.12354

Zhang, W., Jiang, Y., Li, J. Q., Ma, H. G., and Xu, H. L. (2012). Tintinnid ciliates from costal waters off Guangdong, with notes on three new records of China (Protozoa, Ciliophora). *Acta Hydrobiol. Sin.* 36, 744–750.

Zingel, P., Agasild, H., Karus, K., Buholce, L., and Noges, T. (2019). Importance of ciliates as food for fish larvae in a shallow sea bay and a large shallow lake. *Eur. J. Protistol.* 67, 59–70. doi: 10.1016/j.ejop.2018.10.004

Conflict of Interest: The authors declare that the research was conducted in the absence of any commercial or financial relationships that could be construed as a potential conflict of interest.